

Characterization of resonances using finite size effects

B. Pozsgay¹ and G. Takács²

¹*Eötvös University, Budapest*

²*HAS Research Group for Theoretical Physics
H-1117 Budapest, Pázmány Péter sétány 1/A*

13th April 2006

Abstract

We develop methods to extract resonance widths from finite volume spectra of 1+1 dimensional quantum field theories. Our two methods are based on Lüscher's description of finite size corrections, and are dubbed the Breit-Wigner and the improved "mini-Hamiltonian" method, respectively. We establish a consistent framework for the finite volume description of sufficiently narrow resonances that takes into account the finite size corrections and mass shifts properly. Using predictions from form factor perturbation theory, we test the two methods against finite size data from truncated conformal space approach, and find excellent agreement which confirms both the theoretical framework and the numerical validity of the methods. Although our investigation is carried out in 1+1 dimensions, the extension to physical (3+1) space-time dimensions appears straightforward, given sufficiently accurate finite volume spectra.

1 Introduction

Two-dimensional field theories have attracted quite a lot of interest for decades, partly because they are considered to be theoretical laboratories for the development and testing of quantum field theory methods. The present paper can be considered as one more step along this line, taking up the issue of developing methods to extract resonance parameters from finite volume spectra.

The framework of two-dimensional field theory is particularly well adapted to this problem because non-integrable cases are increasingly better understood. In integrable

theories there can exist stable excitations whose decay into lower mass particles would in principle be allowed by their mass and conserved internal charges, but is prevented by the infinitely many integrals of motion underlying integrability. However, by adding a perturbation that breaks integrability one can obtain a much richer phenomenology. At the same time, the underlying integrable model provides us with very powerful tools: firstly, the exact spectrum, scattering theory and form factors at the integrable point are known, and secondly, form factor perturbation theory (FFPT) [1, 2] can give a prediction for the mass shifts, phase shift corrections and decay widths when the non-integrable perturbation is switched on. Therefore the phenomenology is under firm control, which makes these theories into a very convenient testing ground¹.

On the other hand, there exists a rather remarkable tool to compute finite size spectra in two space-time dimensions, known as truncated conformal space approach (TCSA), originally developed in [4] and carried further in many papers, in particular [5, 6, 7].

Recently, Delfino et al. [2] gave a detailed description of the FFPT framework for the decay widths and performed calculations for the Ising model. They also proposed a way to extract the decay width from the finite size spectrum. However, the theoretical relation to the finite volume spectrum was determined incorrectly as we show in section 3.2.1. In addition, they could not reach the required precision to extract any quantitatively useful information from the TCSA spectrum either. In the course of our investigation we also present an improved realization of their proposal which is consistent with a Breit-Wigner resonance description, and demonstrate its quantitative validity using a more advanced TCSA analysis. In addition, we extend our considerations to another prominent example of non-integrable field theory, the double (two-frequency) sine-Gordon model.

We set out to formulate and test methods to extract (partial) decay widths of unstable particles (resonances) from finite volume spectra, using the ideas in [8] as a starting point. In particular we develop new and efficient methods to extract the tiny effects of a narrow resonance with high precision, and test them in the framework provided by two-dimensional quantum field theories. We examine the scaling Ising model with a thermal and magnetic perturbation (i.e. a continuum version of the familiar two-dimensional Ising lattice away from critical temperature and in a magnetic field) and the double (two-frequency) sine-Gordon model, since these are the most studied examples of non-integrable quantum field theories in two dimensions (see the references given in sections 2.2 and 2.3). However, the methods we develop to extract the decay widths are very general, and their higher-dimensional extension seems to be rather straightforward.

The paper is organized as follows. Section 2 introduces the framework of form factor perturbation theory and gives the theoretical predictions for the two models considered. Section 3 is devoted to the theoretical development of the methods used to extract the decay widths from finite volume spectra, and examines the consistency between them. Section

¹It is also possible for resonances to occur in an integrable field theory, as e.g. in the homogeneous sine-Gordon models [3], but the finite volume spectra of these models are not sufficiently understood for the purposes of the present investigation. In addition, the framework of perturbed integrable field theories, in which the decay can be switched on with the integrability breaking perturbation, provides us with a very useful control parameter, i.e. the perturbing coupling, which can be used to tune the resonance width.

4 is devoted to the specification of numerical methods and extrapolation procedures used, and contains a discussion of the sources of numerical errors. We present and discuss our numerical results in section 5, and conclude briefly in section 6. Two technical details are relegated to separate appendices: one is the FFPT derivation of the relevant decay width in the double sine-Gordon model and the other is the detailed calculation performed to examine the consistency of the methods developed in section 3.

2 Unstable particles and form factor perturbation theory

2.1 General formalism

In the framework of conformal perturbation theory, we consider a model with the action

$$\mathcal{A}(\mu, \lambda) = \mathcal{A}_{\text{CFT}} - \mu \int dt dx \Phi(t, x) - \lambda \int dt dx \Psi(t, x) \quad (2.1)$$

such that in the absence of the coupling λ , the model defined by the action $\mathcal{A}(\mu, \lambda = 0)$ is integrable. The two perturbing fields are taken as scaling fields of the ultraviolet limiting conformal field theory, with left/right conformal weights $h_\Phi = \bar{h}_\Phi < 1$ and $h_\Psi = \bar{h}_\Psi < 1$, i.e. they are relevant and have zero conformal spin, resulting in a Lorentz-invariant field theory.

The integrable limit $\mathcal{A}(\mu, \lambda = 0)$ is supposed to define a massive spectrum, with the scale set by the dimensionful coupling μ . The exact spectrum in this case consists of some massive particles, forming a factorized scattering theory with known S matrix amplitudes, and characterized by a mass scale M (which we take as the mass of the fundamental particle generating the bootstrap), which is related to the coupling μ via the mass gap relation

$$\mu = \kappa M^{2-2h_\Phi}$$

where κ is a (non-perturbative) dimensionless constant.

Switching on a second independent coupling λ in general spoils integrability, deforms the mass spectrum and the S matrix, and in particular allows decay of the particles which are stable at the integrable point. One way to approach the dynamics of the model is form factor perturbation theory initiated in [1]. Let us denote the asymptotic states of the $\lambda = 0$ theory by

$$|A_{i_1}(\vartheta_1) \dots A_{i_n}(\vartheta_n)\rangle_{\lambda=0}$$

which describe *in* states if the rapidities are ordered as $\vartheta_1 > \dots > \vartheta_n$ and *out* states for $\vartheta_1 < \dots < \vartheta_n$. Then the essential input to form factor perturbation theory consists of the matrix elements of the local field Ψ (so-called form factors):

$$F_{i_1 \dots i_n}^\Psi(\vartheta_1, \dots, \vartheta_n) = \langle 0 | \Psi(0, 0) | A_{i_1}(\vartheta_1) \dots A_{i_n}(\vartheta_n) \rangle_{\lambda=0}$$

which (due to integrability at $\lambda = 0$) can be obtained in a closed exact form solving the form factor bootstrap axioms and identifying the appropriate solution using known properties of the operator Ψ (for a review of the form factor bootstrap, see [9] and references therein). Given these data the following quantities can be calculated to first order in λ :

1. The vacuum energy density is shifted by an amount

$$\delta\mathcal{E}_{vac} = \lambda \langle 0 | \Psi | 0 \rangle_{\lambda=0}. \quad (2.2)$$

2. The mass (squared) matrix M_{ab}^2 gets a correction

$$\delta M_{ab}^2 = 2\lambda F_{ab}^{\Psi}(i\pi, 0) \delta_{m_a, m_b} \quad (2.3)$$

(where the bar denotes the antiparticle) supposing that the original mass matrix was diagonal and of the form $M_{ab}^2 = m_a^2 \delta_{ab}$.

3. The scattering amplitude for the four particle process $a + b \rightarrow c + d$ is modified by

$$\delta S_{ab}^{cd}(\vartheta, \lambda) = -i\lambda \frac{F_{cdab}^{\Psi}(i\pi, \vartheta + i\pi, 0, \vartheta)}{m_a m_b \sinh \vartheta}, \quad \vartheta = \vartheta_a - \vartheta_b. \quad (2.4)$$

It is very important to keep in mind that this gives the variation of the scattering phase when the center-of-mass energy (or, the Mandelstam variable s) is kept fixed [1]. Therefore, in terms of rapidity variables, this variation corresponds to the following:

$$\delta S_{ab}^{cd}(\vartheta, \lambda) = \frac{\partial S_{ab}^{cd}(\vartheta, \lambda = 0)}{\partial \vartheta} \delta \vartheta + \lambda \left. \frac{\partial S_{ab}^{cd}(\vartheta, \lambda)}{\partial \lambda} \right|_{\lambda=0}$$

where

$$\delta \vartheta = - \frac{m_a \delta m_a + m_a \delta m_a + (m_b \delta m_a + m_a \delta m_b) \cosh \vartheta}{m_a m_b \sinh \vartheta}$$

is the shift of the rapidity variable induced by the mass corrections (2.3).

It is not yet clear how to extend these results to second order. However, it is possible to calculate the (partial) decay width of particles [2]. Suppose that the decay of particle A_c into particles A_a and A_b is kinematically allowed: $m_c > m_a + m_b$. Then in the rest frame of particle A_c the rapidities of the outgoing particles are uniquely determined from energy-momentum conservation

$$\begin{aligned} m_a \sinh \vartheta_a^{(cab)} + m_b \sinh \vartheta_b^{(cab)} &= 0 \\ m_a \cosh \vartheta_a^{(cab)} + m_b \cosh \vartheta_b^{(cab)} &= m_c \end{aligned}$$

and the partial decay width can be calculated as

$$\Gamma_{c \rightarrow ab} = \lambda^2 2^{1-\delta_{ab}} \frac{|F_{cab}^{\Psi}(i\pi, \vartheta_a^{(cab)}, \vartheta_b^{(cab)})|^2}{m_c^2 m_a |\sinh \vartheta_a^{(cab)}|} \quad (2.5)$$

All the masses m_a in the above formulae correspond to those in the unperturbed ($\lambda = 0$) theory.

2.2 Thermal perturbation of Ising model with magnetic field

The action

$$\mathcal{A}_{\text{Ising}}(h, \tau) = \mathcal{A}_{c=\frac{1}{2}} - h \int dt dx d\sigma(t, x) - \tau \int dt dx \epsilon(t, x) \quad (2.6)$$

describes the two-dimensional scaling Ising model, where $\mathcal{A}_{c=\frac{1}{2}}$ is the action of the $c = 1/2$ conformal field theory (free massless Majorana fermion), describing the conformal limit of the two-dimensional Ising model, ϵ is the energy density operator (which is a primary field of weight $\Delta_\epsilon = \bar{\Delta}_\epsilon = 1/2$) and σ is the magnetization operator ($\Delta_\sigma = \bar{\Delta}_\sigma = 1/16$). The coupling h corresponds to the applied external magnetic field and τ parameterizes the deviation of the temperature from criticality². This model is considered as a prototype non-integrable field theory in [1] and is widely discussed in the literature [11, 12, 13, 14]. There are two options to consider it as a perturbed integrable field theory. One way is to take h as the perturbing coupling: in this case the Majorana fermions of the thermally perturbed Ising model can be demonstrated to go through some sort of confinement (McCoy-Wu scenario [15]), and the decay widths of the high-lying “meson” states were computed to $O(h^3)$ in [16]. Here we take the opposite route and consider τ as the coupling that breaks integrability.

For $\tau = 0$ the spectrum and the exact S matrix is described by the famous E_8 factorized scattering theory [17], which contains eight particles A_i , $i = 1, \dots, 8$ with mass ratios given by

$$\begin{aligned} m_2 &= 2m_1 \cos \frac{\pi}{5} \\ m_3 &= 2m_1 \cos \frac{\pi}{30} \\ m_4 &= 2m_2 \cos \frac{7\pi}{30} \\ m_5 &= 2m_2 \cos \frac{2\pi}{15} \\ m_6 &= 2m_2 \cos \frac{\pi}{30} \\ m_7 &= 2m_4 \cos \frac{\pi}{5} \\ m_8 &= 2m_5 \cos \frac{\pi}{5} \end{aligned}$$

and the mass gap relation is [18]

$$m_1 = (4.40490857\dots)|h|^{8/15}$$

or

$$h = \kappa_h m_1^{8/15}, \quad \kappa_h = 0.06203236\dots \quad (2.7)$$

²Note that for this model the notation for the couplings is changed from μ, λ to h, τ in order to conform with the notations used in [2]. In addition, Φ is now σ and Ψ is ϵ .

We also quote the scattering phase shift of two A_1 particles for $\lambda = 0$, which has the form

$$S_{11}(\vartheta) = \left\{ \frac{1}{15} \right\} \left\{ \frac{1}{3} \right\} \left\{ \frac{2}{5} \right\} \quad , \quad \{x\} = \frac{\sinh \vartheta + i \sin \pi x}{\sinh \vartheta - i \sin \pi x} \quad (2.8)$$

All the other amplitudes S_{ab} are determined by the S matrix bootstrap [17].

The non-integrable model (2.6) has a single dimensionless parameter, which we choose as

$$t = \frac{\tau}{|h|^{8/15}}$$

The form factors of the operator ϵ in the E_8 model were first calculated in [19] and their determination was carried further in [2]. Using the exact form factor solutions the following results were obtained in [2] for the mass shift of A_a and the partial decay width associated to $A_c \rightarrow A_a + A_b$:

$$\begin{aligned} \delta m_a^2 &= 2\tau f_{aa} \\ \Gamma_{c \rightarrow a+b} &= \tau^2 2^{1-\delta_{ab}} \frac{f_{cab}^2}{m_c^2 m_a \sinh \vartheta_a^{(cab)}} \end{aligned}$$

where

$$\begin{aligned} f_{11} &= (-17.8933\dots)\langle\epsilon\rangle \\ f_{22} &= (-24.9467\dots)\langle\epsilon\rangle \\ f_{33} &= (-53.6799\dots)\langle\epsilon\rangle \\ f_{44} &= (-49.3206\dots)\langle\epsilon\rangle \\ f_{411} &= (36.73044\dots)\langle\epsilon\rangle \\ f_{511} &= (19.16275\dots)\langle\epsilon\rangle \\ f_{512} &= (11.2183\dots)\langle\epsilon\rangle \end{aligned}$$

and the vacuum expectation value of the perturbing field ϵ for $\tau = 0$ is given by [20]

$$\langle\epsilon\rangle = \epsilon_h |h|^{8/15} \quad , \quad \epsilon_h = 2.00314\dots$$

The dimensionless decay width for the processes $A_c \rightarrow A_1 + A_1$, $c = 4, 5$ can be written as

$$\frac{\Gamma_{c \rightarrow 11}}{m_1} = t^2 \frac{(\epsilon_h \kappa^{16/15} f'_{c11})^2}{\left(\frac{m_c}{m_1}\right)^2 \sqrt{\left(\frac{m_c}{2m_1}\right)^2 - 1}} \quad , \quad c = 4, 5 \quad (2.9)$$

where

$$\begin{aligned} f'_{411} &= 36.73044\dots \\ f'_{511} &= 19.16275\dots \end{aligned}$$

2.3 Double (two-frequency) sine-Gordon model

Double sine-Gordon theory is another prototype of non-integrable field theories which can be understood by application of techniques developed in the context of integrable models [10]. It has several interesting applications e.g. to the study of massive Schwinger model (two-dimensional quantum electrodynamics), and in the description of a generalized Ashkin-Teller model (a quantum spin system), both of which are discussed in [10]. Another application to the one-dimensional Hubbard model is examined in [21] (together with the generalized Ashkin-Teller model mentioned above). A further potentially interesting application of the two-(and multi-)frequency sine-Gordon model is the description of ultra-short optical pulses propagating in resonant degenerate medium [22]. Its phase diagram was studied using non-perturbative finite size techniques in [23], and the results were recently extended to the multi-frequency generalization in [24]. There has been a certain doubt concerning the validity of factor perturbation theory (or rather the proper way of performing it) after Mussardo et al. [25] applied a semiclassical soliton form factor technique developed by Goldstone and Jackiw [26], and obtained results that contradict explicitly some of the results derived from standard form factor perturbation theory in [23]. However, the conclusions drawn from the semiclassical technique were shown to be untenable by extensive numerical work in [27], which upheld the results of form factor perturbation theory as applied in [23], and therefore we follow the same approach in this paper.

The action of the two-frequency sine-Gordon model (with frequency ratio 1 : 2) is

$$\begin{aligned} \mathcal{A} &= \mathcal{A}_{c=1} + \mu \int dt dx \cos \beta \varphi + \lambda \int dt dx \cos \left(\frac{\beta}{2} \varphi + \delta \right) \\ \mathcal{A}_{c=1} &= \int dt dx \frac{1}{2} (\partial \varphi)^2 \end{aligned} \quad (2.10)$$

The spectrum at $\lambda = 0$ consists of a soliton doublet with mass M related to μ via [28]

$$\begin{aligned} \mu &= \kappa_{\text{sG}}(\xi) M^{2/(\xi+1)} \\ \kappa_{\text{sG}}(\xi) &= \frac{2\Gamma(\frac{\xi}{1+\xi})}{\pi\Gamma(\frac{\xi}{1+\xi})} \left(\frac{\sqrt{\pi}}{2\Gamma(\frac{\xi+1}{2\xi})\Gamma(\frac{\xi}{2})} \right)^{2/(\xi+1)}, \quad \xi = \frac{\beta^2}{8\pi - \beta^2} \end{aligned} \quad (2.11)$$

and breathers B_n with masses

$$m_n = 2M \sin \frac{n\pi\xi}{2}, \quad n = 1, \dots, [1/\xi] \quad (2.12)$$

The exact S matrix of all these particles was derived from the axioms of factorized scattering in [29].

The strength of the non-integrable perturbation can be characterized using the dimensionless ratio

$$t = \frac{\lambda}{M^{\frac{4+3\xi}{2+2\xi}}}$$

where M is the soliton mass at the integrable point $\lambda = 0$. From (2.12)

$$\frac{m_3}{m_1} = 1 + 2 \cos \pi \xi > 2 \quad \text{if} \quad \xi < 1/3$$

so whenever B_3 exists, its decay to 2 B_1 -s is always kinematically allowed (for λ small enough) and the same holds for all the B_n , $n \geq 3$. However, since

$$\frac{m_2}{m_1} = 2 \cos \frac{\pi \xi}{2} < 2$$

B_2 cannot decay to a pair of B_1 -s (and therefore cannot decay at all) if the perturbation λ and correspondingly the mass shifts are small enough. The decay width corresponding to the simplest process $B_3 \rightarrow B_1 + B_1$ is calculated in Appendix A for $\delta = -\pi/2$. The dimensionless decay width can be written as

$$\frac{\Gamma_{3 \rightarrow 11}}{M} = t^2 \frac{s_{311}^2}{\left(\frac{m_3}{M}\right)^2 \frac{m_1}{M} \sqrt{\left(\frac{m_3}{2m_1}\right)^2 - 1}} \quad (2.13)$$

where s_{311} is given by (A.7). Because the B_3 state is the lowest one whose decay can be observed, it is preferable to use in the comparison with truncated conformal space to minimize the truncation errors. In addition, there is a \mathbb{Z}_2 symmetry at $\delta = -\pi/2$ which can be turned to a significant numerical advantage (see the analysis in subsection 4.1 for details).

3 Resonance widths from finite volume spectra

In this section we discuss two different approaches to linking the finite volume spectra with the theoretical predictions of form factor perturbation theory in the previous section. The first one uses a Breit-Wigner parameterization for the finite volume levels in the vicinity of the volume L_0 where the one particle level A_c crosses the two-particle level $A_a A_b$ before switching on the coupling. This method relies on obtaining the two particle phase shift from the finite size spectrum using Lüscher's results [30] and then finding the Breit-Wigner resonance parameters directly from the phase shift. The second approach uses a “mini-Hamiltonian” description for the levels to extract directly the form factor determining the decay width. The two approaches are then compared and we learn how to improve the results of Delfino et al. [2] for the “mini-Hamiltonian” to make them consistent with the Breit-Wigner description (for a narrow resonance).

3.1 Lüscher's formulation: methods to extract the decay rate from the finite size spectrum

Suppose that the finite volume spectrum of the theory is given in a form of functions $E_i(L)$ describing the energy of the i th excited state as a function of volume L , normalized to

the ground state energy in the same volume. Suppose further that we investigate a decay process $A_c \rightarrow A_a + A_b$ ($m_c > m_a + m_b$) and that we have a parameter λ describing the interaction responsible for the decay, such that for $\lambda = 0$ the particle A_c is stable (the notation here follows the conventions of section 2.1).

We can then find the energy level corresponding asymptotically to a stationary particle A_c at $\lambda = 0$, denoted by $E_c(L)$ and two-particle levels composed of A_a and A_b with zero total momentum, denoted by $E_{ab}(L)$ (where we suppressed an index labeling states corresponding to different relative momenta of a and b). According to [30], up to corrections vanishing exponentially with L (which we neglect from now on), the finite size correction to the two-particle level is determined by the equations

$$\begin{aligned} m_a L \sinh \vartheta_a + \delta_{ab}(\vartheta_a - \vartheta_b) &= 2n_a \pi \\ m_b L \sinh \vartheta_b + \delta_{ab}(\vartheta_b - \vartheta_a) &= 2n_b \pi \end{aligned} \quad (3.1)$$

and

$$E_{ab}(L) = m_a \cosh \vartheta_a + m_b \cosh \vartheta_b$$

where $\delta_{ab}(\vartheta) = -\delta_{ab}(-\vartheta)$ is the elastic two-particle phase shift defined from the elastic two-particle scattering phase S_{ab} via the relation

$$S_{ab}(\vartheta) = e^{i\delta_{ab}(\vartheta)}$$

and $n = n_a = -n_b$ for zero total momentum labels the different possible values for the relative momentum. As a result, the energy of any two particle level decreases as $1/L^2$, while the finite size corrections of a one-particle level are known to vanish exponentially fast with increasing volume [31]. In the infinite volume limit $E_{ab}(L) < E_c(L)$ (since in the limit $L \rightarrow \infty$ they tend to $m_a + m_b$ and m_c , respectively) and therefore there is a volume L_0 where the two levels meet: $E_{ab}(L_0) = E_c(L_0) = E_0$.

3.1.1 The “mini-Hamiltonian”

Switching on a small $\lambda \neq 0$ the levels only move a small amount and thus can be easily re-identified, however the degeneracy at L_0 is lifted by an amount related to the width of the decay process (as we shall see shortly). Let us restrict ourselves to the two-dimensional subspace spanned by the two levels. We suppose that the relevant region in the volume L is of order λ , which turns out to be a self-consistent assumption. Then for $L \sim L_0$ and $\lambda \sim 0$ the effective “mini-Hamiltonian” in this subspace which determines the behaviour of the levels to leading order in $L - L_0$ and λ can be parameterized as follows

$$H = E_0 + (L - L_0) \begin{pmatrix} \alpha_1 & \\ & \alpha_2 \end{pmatrix} + \lambda \begin{pmatrix} A(L) & B(L) \\ B(L) & C(L) \end{pmatrix} \quad (3.2)$$

where the relative phases of the two states were chosen such that B is real and nonnegative (A, C are real by hermiticity). According to the prescription of degenerate perturbation

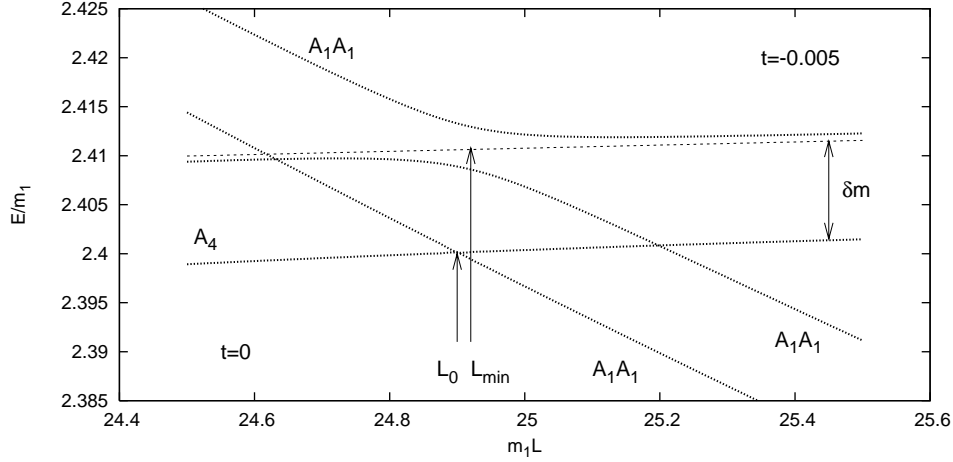


Figure 3.1: Behaviour of levels at $\lambda = 0$ and $\lambda \neq 0$, illustrated using actual numerical data for the Ising case. (Energy and distance are measured in units given by the value that the mass of the lightest particle (m_1) takes at $\lambda = 0$.)

theory, the splitting of the two levels is given by diagonalizing (3.2) in the subspace of the two levels:

$$\delta E(L) = \sqrt{((\alpha_1 - \alpha_2)(L - L_0) + \lambda(A(L) - C(L)))^2 + 4B^2\lambda^2}$$

Neglecting the volume dependence of A , B and C for the moment, the minimum splitting between the two levels occurs at

$$L_{\min} - L_0 = -\lambda \frac{A - C}{\alpha_1 - \alpha_2} \quad (3.3)$$

which shows that it was consistent to suppose that the relevant values of $L - L_0$ are of the order λ . The minimal energy split is then

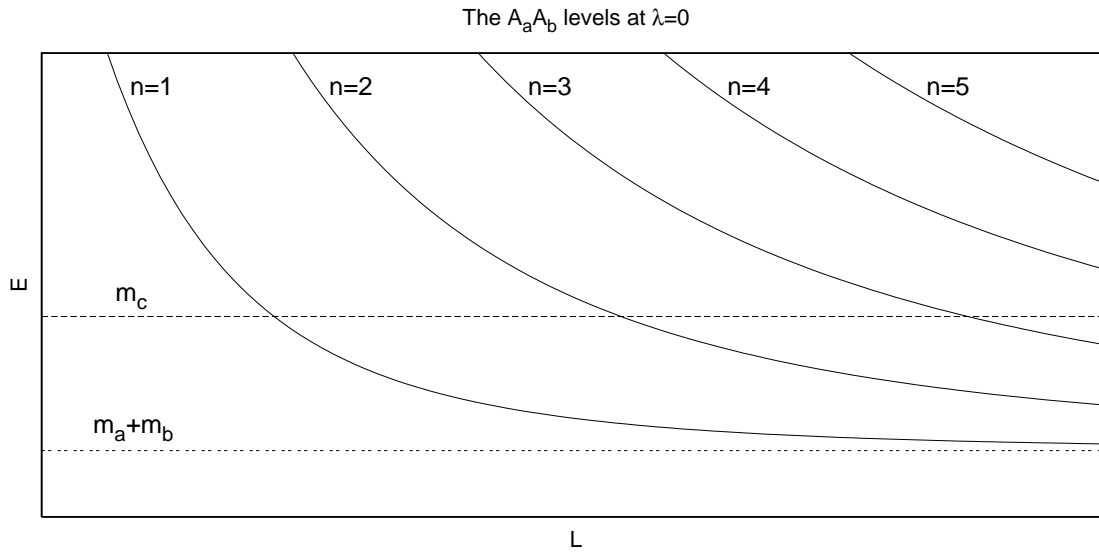
$$\delta E(L_{\min}) = 2|B\lambda| \quad (3.4)$$

This shows that to first order in λ it is consistent to replace the coefficients $A(L)$, $B(L)$, $C(L)$ by their values taken at L_0 . This observation will be used several times in the sequel.

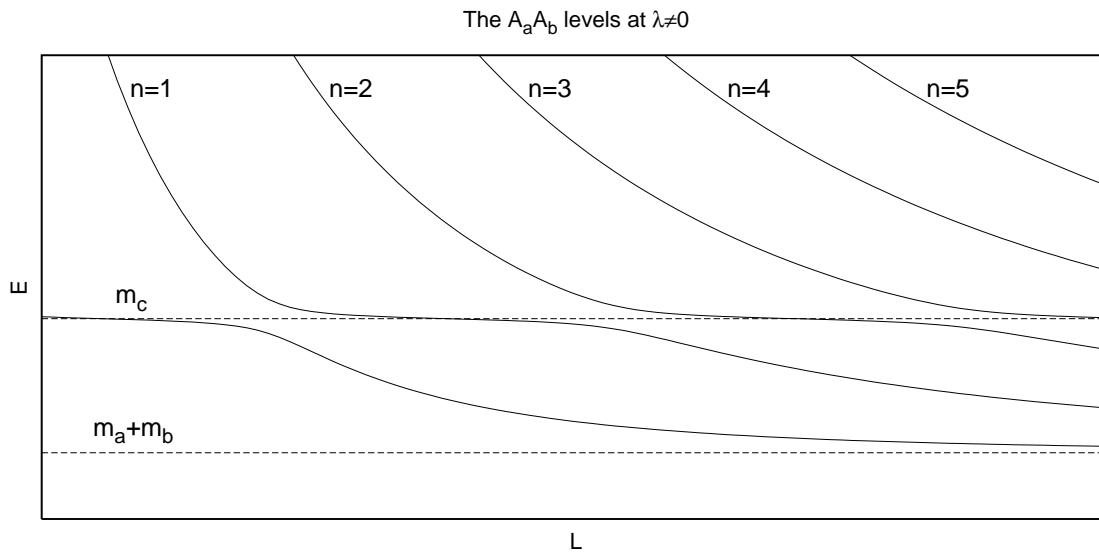
The behaviour of levels discussed above is illustrated in figure 3.1.

3.1.2 Breit-Wigner analysis

Here we build on the approach advocated by Lüscher in [8], but with some modification to make it more suited to numerical analysis. At $\lambda \neq 0$ there are no stable one-particle states of A_c anymore, and therefore asymptotically all the states are identified as two-particle states $A_a A_b$. Due to the lifting of the degeneracies in the crossings with the one-particle



(a) $\lambda = 0$



(b) $\lambda \neq 0$

Figure 3.2: Illustrating the behaviour of two-particle states in the integrable case $\lambda = 0$ and with a resonance present ($\lambda \neq 0$).

level of A_c these states acquire plateaux as illustrated in figure 3.2, which correspond to the appearance of a Breit-Wigner resonance contribution in the two-particle phase shift:

$$\delta_{ab}(E) = \delta_0(E) + \delta_{BW}(E)$$

(as a function of the center-of-mass energy E), where δ_0 is the background part of the phase shift, and the Breit-Wigner contribution has the form

$$\delta_{BW}(E) = -i \log \frac{E - E_c - i\Gamma/2}{E - E_c + i\Gamma/2}$$

with E_c as the center and Γ as the width of the resonance. If

$$\beta = \left. \frac{d\delta_0}{dE} \right|_{E=E_c} < 0$$

then the total phase shift has two extrema (a minimum at $E < E_c$ and a maximum at $E > E_c$, see figure 3.3). Their positions can be calculated to first order in Γ :

$$E_{\pm} = E_c \pm \sqrt{-\frac{\Gamma}{\beta}}$$

with the values

$$\delta_{ab}(E_{\pm}) = \pi + \delta_0(E_c) \pm \left(\pi - 2\sqrt{-\beta\Gamma} \right)$$

Now let us take two neighbouring two-particle levels $E_1(L)$ and $E_2(L)$. Using the description (3.1) we can define the phase shift functions for the two levels as follows: first solve

$$E = \sqrt{p^2 + m_a^2} + \sqrt{p^2 + m_b^2} \rightarrow p(E)$$

and then extract the phase shift as

$$\begin{aligned} \delta_1(E) &= -L_1(E)p(E) \\ \delta_2(E) &= -L_2(E)p(E) \end{aligned} \tag{3.5}$$

where $L_{1,2}(E)$ are the volume-energy functions for the two states (here we supposed that the two-particle state has zero total momentum, and the momenta of the particles are p and $-p$). The functions $\delta(E)$ are illustrated in figure 3.3. Since

$$\begin{aligned} \delta_1(E) &= \delta_{ab}(E) - 2n_1\pi \\ \delta_2(E) &= \delta_{ab}(E) - 2n_2\pi \end{aligned}$$

where n_1 and n_2 are the momentum quantum numbers which for neighbouring states satisfy $n_2 = n_1 + 1$, we obtain

$$\Delta\delta = \min \delta_1(E) - \max \delta_2(E) = 4\sqrt{-\beta\Gamma} \tag{3.6}$$

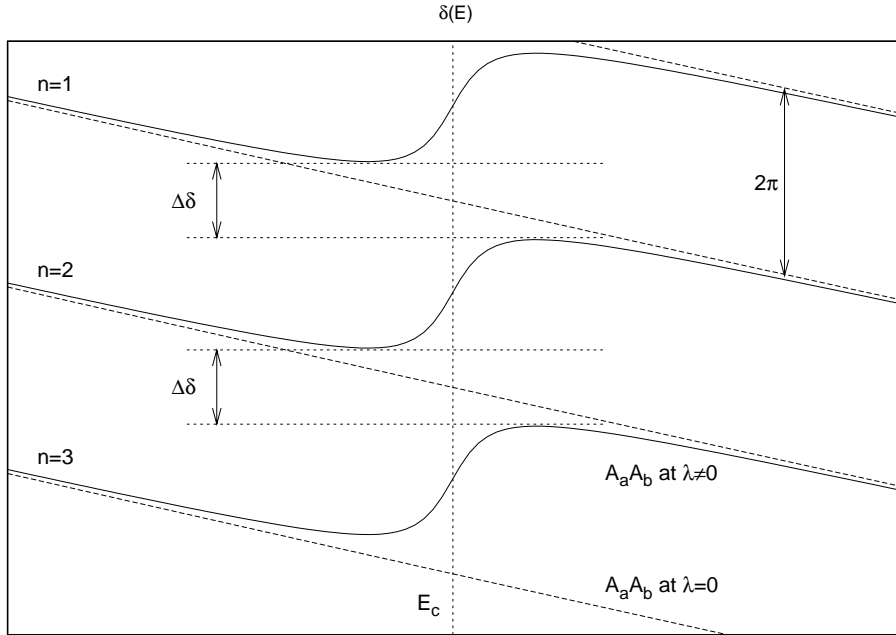


Figure 3.3: Phase shift functions $\delta_n(E)$ extracted from the two-particle levels illustrated in figure 3.2 around the resonant energy E_c .

This gives a method to extract the value of Γ from the finite volume spectrum: determine first the phase shift functions $\delta_{1,2}$ from two neighbouring two-particle levels and then take the difference between their extrema to find $\sqrt{\Gamma}$. Since Γ is of order λ^2 , it follows that $\sqrt{\Gamma}$ is of order λ which means that it is much easier to measure than Γ in the small λ regime when the resonance is narrow. This is a huge advantage over previously proposed methods which gave Γ directly, like the approach advocated in [8] which relates Γ to the slope of the plateaux at their middle point (more precisely at the value of the volume when the resonant contribution to the phase shift δ of the given level passes through π). Indeed it is already apparent from figure 3.2 that the level splittings determining Δ are much easier to observe compared to the slope at the middle of the plateaux. In addition, Δ can be extracted by measuring the spectrum in a small neighbourhood of L_{\min} which makes the *residual* finite size effects (those that decay exponentially on the volume) much easier to control.

Finally we remark that while the simplest possibility of extracting the resonance parameters would seem to be the method of fitting the numerically determined phase shift function $\delta(E)$ with a Breit-Wigner resonance function, in practice this has the severe disadvantage that the finite size data necessary to extract the relevant part of the phase shift cover an extended range between two line crossings together with a neighbourhood of the crossings themselves. Over such an extended range, the contribution of residual finite size corrections varies substantially, which causes such a significant distortion of the shape of

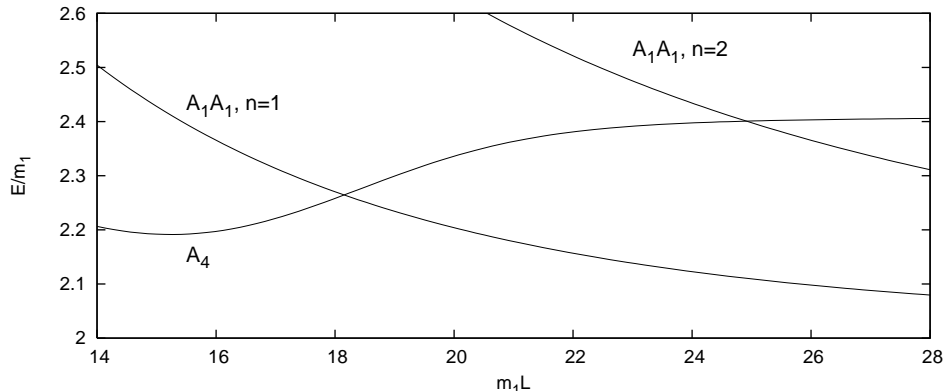


Figure 3.4: Illustration of the residual finite size effects in the Ising model, for the levels pertaining to A_4 and two-particle states $A_1 A_1$. The volume dependence of the two-particle levels follows very precisely the description given in eq. (3.1), but the variation of A_4 is entirely due to the residual finite size effects that we neglected. The plot shows the integrable case $t = 0$ when the line crossings are exact, but the only result of switching on a small value for t is a slight shift in the lines and resolution of the degeneracy at the level crossings.

the Breit-Wigner resonance contribution that there is no way to perform a reliable fit to the data. This problem is illustrated in figure 3.4, where it is obvious how much the one-particle level varies between two adjacent level crossings. This also makes the application of Lüscher’s “plateau slope” method impossible, which can be seen from the fact that in the absence of residual finite size effects we would expect the slope to be negative, as illustrated in figure 3.2. However, it is obvious from the data in figure 3.4 that the leading residual finite size corrections are such that the particle masses approach their infinite volume from below, which is known to be a generic feature in two dimensional field theories [33].

3.1.3 Linking the “mini-Hamiltonian” with the Breit-Wigner formula

We can now match this method with the previous one. For simplicity we shall assume that the two decay products are identical to a particle denoted by A_1 (i.e. $a = b = 1$). Parameterizing the two levels using (3.2) we can express the parameters in the “mini-Hamiltonian” by extracting

$$\Delta\delta = \min \delta_1(E) - \max \delta_2(E)$$

from the levels and matching it with the result (3.6) of the Breit-Wigner analysis. From (3.2), the two levels read

$$E_{1,2} = E_0 + \frac{A+C}{2}\lambda + \frac{1}{2}(\alpha_1 + \alpha_2)(L - L_0) \pm \frac{1}{2}\sqrt{(\alpha_1 - \alpha_2)^2(L - L_{\min})^2 + 4B^2\lambda^2}$$

(E_1/E_2 corresponds to the sign choice $+/-$, respectively) where L_{\min} is given by eq. (3.3). At $\lambda = 0$

$$E_{1,2} = E_0 + \frac{1}{2}(\alpha_1 + \alpha_2)(L - L_0) \pm \frac{1}{2}(\alpha_1 - \alpha_2)|L - L_0|$$

Recalling that m_c is the mass of the particle A_c whose decay process we are interested in, we get $E_0 = m_c$ (where we neglected the residual finite size effects decaying exponentially with the volume, as before). Furthermore, it is known that $E_2 = m_c$ for $L < L_0$ and $E_1 = m_c$ at $L > L_0$ (due to the level crossing at L_0 , the interpretation of the levels in terms of asymptotic particle states swaps over). As a result, $\alpha_1 = 0$ and $\alpha_2 = -2\alpha < 0$, and so the expression for the two levels turns into

$$E_{1,2} = m_c + A\lambda - \alpha(L - L_{\min}) \pm \sqrt{\alpha^2(L - L_{\min})^2 + B^2\lambda^2} \quad (3.7)$$

with

$$L_{\min} = L_0 - \lambda \frac{A - C}{2\alpha} \quad (3.8)$$

and denoting

$$A = A(L_0) \quad , \quad B = B(L_0) \quad , \quad C = C(L_0)$$

since as pointed out in section 3.1.1, the coefficients $A(L), B(L), C(L)$ can be substituted with their values taken at $L = L_0$ if one calculates only to the lowest order in λ .

Note that for $|\alpha(L - L_{\min})| \gg |B\lambda|$ one of the levels (the identity of which depends on the sign of $L - L_{\min}$) is L -independent and takes the value

$$E_c(\lambda) = m_c + A\lambda \quad (3.9)$$

which therefore can be identified with the mass of the resonance corresponding to the unstable particle A_c , to first order in λ (this shift is also illustrated in figure 3.1).

Using form factor perturbation theory (2.3) we obtain the identification

$$A = \frac{f_{cc}}{m_c} \quad , \quad f_{cc} = F_{cc}(i\pi, 0).$$

After some calculation (the details are given in Appendix B) the phase shift difference can also be extracted

$$\min \delta_1 - \max \delta_2 = 2B\lambda \sqrt{-\frac{1}{\alpha} \sqrt{m_c^2 - 4m_1^2} \frac{d\delta_0}{dE} \Big|_{E=E_0}}$$

where $\delta_{1,2}$ are the phase shift functions for the levels $E_{1,2}(L)$ as defined in (3.5). Now this must be compared to the result from the Breit-Wigner analysis (cf. eq. (3.6))

$$\min \delta_1 - \max \delta_2 = 4 \sqrt{-\Gamma \frac{d\delta_0}{dE} \Big|_{E=E_0}}$$

This way we obtain the relation

$$\Gamma = \frac{B^2 \lambda^2}{4\alpha} \sqrt{m_c^2 - 4m_1^2}$$

On the other hand, using the form factor perturbation theory result (2.5) gives

$$\Gamma = \lambda^2 \frac{f_{c11}^2}{m_c^2 m_1 \left| \sinh \vartheta_1^{(c11)} \right|} \quad , \quad f_{c11} = \left| F_{c11}^\Psi \left(i\pi, \vartheta_1^{(c11)}, \vartheta_1^{(c11)} \right) \right|$$

$$m_c = 2m_1 \cosh \vartheta_1^{(c11)}$$

and so

$$B = \frac{f_{c11}}{m_c} \sqrt{\frac{8\alpha}{m_c^2 - 4m_1^2}}$$

We also need an expression for α . At $\lambda = 0$ we can express it using the energy $E_{11}(L)$ of the $A_1 A_1$ two-particle state from (B.2)

$$\alpha = -\frac{1}{2} \frac{dE_{11}}{dL} \Big|_{L=L_0}$$

Writing the energy of the two-particle level with the one-particle momentum p as $E_{11}(L) = 2\sqrt{p(L)^2 + m_1^2}$ and using $E_{11}(L_0) = m_c + O(\lambda)$ we get

$$B = \frac{2f_{c11}}{m_c^{3/2}} \sqrt{\left(-\frac{1}{p} \frac{dp(L)}{dL} \right) \Big|_{L=L_0}} \quad (3.10)$$

Putting $B = 0$ the level corresponding to the two-particle state $A_1 A_1$ takes the following value at L_0 :

$$E_{11}(L_0) = m_c + C\lambda$$

so $C\lambda$ is the energy shift of the two-particle level at the volume $L = L_0$ if the resonance contribution is neglected. This is also consistent with eq. (3.8) which for $B = 0$ gives the location of the level crossing to first order in λ . This observation provides a possibility to determine C (for details see Appendix C.1), with the result

$$C = \left(-\frac{1}{p} \frac{dp(L)}{dL} \right) \Big|_{L=L_0} \left(\frac{4f_{1111}}{m_c^2} + L_0 \frac{4f_{11}}{m_c} \right) \quad (3.11)$$

3.2 Theoretical determination of the “mini-Hamiltonian”

3.2.1 Mismatch between the Breit-Wigner formalism and the DGM prediction

Now let us turn to theoretical determination of the “mini-Hamiltonian” (3.2)

$$H = E_0 + (L - L_0) \begin{pmatrix} \alpha_1 & \\ & \alpha_2 \end{pmatrix} + \lambda \begin{pmatrix} A(L) & B(L) \\ B(L) & C(L) \end{pmatrix}$$

It was shown in subsection 3.1.3 that matching the “mini-Hamiltonian description” with the Breit-Wigner analysis gives the relations

$$A_{\text{BW}}(L_0) = \frac{f_{cc}}{m_c} \quad , \quad B_{\text{BW}}(L_0) = \frac{2f_{c11}}{m_c^{3/2}} \sqrt{\left(-\frac{1}{p} \frac{dp(L)}{dL} \right) \Big|_{L=L_0}} \quad (3.12)$$

In addition, matching the Lüscher description (3.1) of the two-particle states with the “mini-Hamiltonian” also gave (3.11) for C .

Delfino, Grinza and Mussardo (DGM for short) obtain the following results for the matrix elements [2]

$$A_{\text{DGM}}(L) = \frac{f_{cc}}{m_c} \quad , \quad B_{\text{DGM}}(L) = \frac{2f_{c11}}{\sqrt{m_c^3 L}} \quad , \quad C_{\text{DGM}}(L) = \frac{4f_{1111}}{m_c^2 L} \quad (3.13)$$

where

$$f_{cc} = F_{c\bar{c}}^\Psi(i\pi, 0) \quad , \quad f_{1111} = \lim_{\delta \rightarrow 0} F_{1111}^\Psi \left(\vartheta_1^{(c11)} + i\pi - \delta, -\vartheta_1^{(c11)} + i\pi - \delta, -\vartheta_1^{(c11)}, \vartheta_1^{(c11)} \right) \quad (3.14)$$

and

$$f_{c11} = \left| F_{c11}^\Psi \left(i\pi, \vartheta_1^{(c11)}, \vartheta_1^{(c11)} \right) \right| \quad (3.15)$$

(recall that the phase of the matrix element $B(L)$ can be transformed away by redefining the relative phase of the two states, so we can take the absolute value in (3.15)).

We can see that the result for $A(L_0)$ matches perfectly, but $B(L_0)$ agrees only if

$$\left(-\frac{1}{p} \frac{dp(L)}{dL} \right) \Big|_{L=L_0} = \frac{1}{L_0}$$

This is only true if we neglect the background phase shift δ_0 since the quantization rule for the momentum is

$$\begin{aligned} pL + \delta_0(E) &= 2n\pi \\ E &= 2\sqrt{p^2 + m_1^2} \end{aligned}$$

Putting $\delta_0 = 0$

$$p(L) = \frac{2n\pi}{L} \quad \Rightarrow \quad \left(-\frac{1}{p} \frac{dp(L)}{dL} \right) \Big|_{L=L_0} = \frac{1}{L_0}$$

However, the background phase shift is already present at $\lambda = 0$ and therefore the formulae (3.13) are not consistent with the Breit-Wigner analysis to first order in λ . In fact, the

background phase shift (especially the fact that $\delta'_0(E_0) < 0$) played an important role in the considerations based on the Breit-Wigner resonance parameterization.

In addition, the DGM prediction for C does not agree with (3.11) and so is inconsistent with the behaviour of two-particle states in finite volume even in the absence of a resonance. Taken together, this means that the DGM formulae (3.13) cannot be used self-consistently to extract the form factors from the behaviour of the levels for small λ .

3.2.2 Rederiving the “mini-Hamiltonian” from the Lagrangian approach

We shall now resolve the above problem by reexamining the derivation of the “mini-Hamiltonian” from the Lagrangian approach. We normalize the one-particle states in infinite volume as

$$\langle A_a(p_a) | A_b(p_b) \rangle = 2\pi \delta_{ab} \delta(p_a - p_b) E_a$$

In finite volume the one-particle momenta (up to corrections vanishing exponentially with the volume) are quantized as

$$p_a = \frac{2\pi n_a}{L}$$

with the density of states

$$\frac{dn}{dp} = \frac{L}{2\pi}$$

therefore the normalization reads

$$\langle A_a(p_a) | A_b(p_b) \rangle = \delta_{ab} \delta_{p_a p_b} L E_a$$

To obtain an orthonormal basis the one-particle states in finite volume must be related to the ones in infinite volume as

$$|A_a(p_a)\rangle_L = \frac{1}{\sqrt{E_a L}} |A_a(p_a)\rangle$$

The normalization of two-particle states in infinite volume reads

$$\langle A_a(p_a) A_b(p_b) | A_c(p_c) A_d(p_d) \rangle = 2\pi \delta_{ac} \delta(p_a - p_c) E_a 2\pi \delta_{bd} \delta(p_b - p_d) E_b$$

Taking the density of the two-particle states to be the product of the one-particle densities, the following expression is obtained for the states normalized in finite volume L

$$|A_a(p_a) A_b(p_b)\rangle_L = \frac{1}{\sqrt{E_a L}} \frac{1}{\sqrt{E_b L}} |A_a(p_a) A_b(p_b)\rangle$$

In particular, considering states containing two identical particles and having zero total momentum we get

$$|A_a(p_a) A_a(-p_a)\rangle_L = \frac{2}{EL} |A_a(p_a) A_a(-p_a)\rangle$$

where $E = 2E_a$ is the total energy of the state. The perturbing operator reads

$$H' = \lambda \int_0^L dx \Psi(x)$$

The mini-Hamiltonian can be computed taking the matrix elements of H' in the basis

$$|A_c(0)\rangle_{L=L_0} \quad , \quad |A_1(p)A_1(-p)\rangle_{L=L_0}$$

Using translational invariance to perform the spatial integration, and the fact that the energy of these states is $E_c(L_0) = E_{11}(L_0) = m_c$ the expression of the “mini-Hamiltonian” in terms of the form factors in infinite volume becomes

$$\begin{aligned} A(L_0) &= L_0 \frac{1}{m_c L_0} \langle A_c(0) | \Psi(0) | A_c(0) \rangle = \frac{f_{cc}}{m_c} \\ B(L_0) &= L_0 \frac{2}{(m_c L_0)^{3/2}} \langle A_c(0) | \Psi(0) | A_1(p) A_1(-p) \rangle = \frac{2f_{c11}}{\sqrt{m_c^3 L_0}} \\ C(L_0) &= L_0 \frac{4}{(m_c L_0)^2} \langle A_1(p) A_1(-p) | \Psi(0) | A_1(p) A_1(-p) \rangle = \frac{4f_{1111}}{m_c^2 L_0} + \frac{4f_{11}}{m_c} \end{aligned} \quad (3.16)$$

where

$$f_{11} = F_{11}^\Psi(i\pi, 0)$$

$A(L_0)$ and $B(L_0)$ does agree with the DGM result (3.13), but $C(L_0)$ contains a new term coming from the disconnected part of the four-particle matrix element. The origin of this contribution is that in contrast to the bulk setting discussed in [1], the finite volume Hamiltonian does not include any counter terms for the mass shifts (for details see Appendix C.2). The presence of the disconnected term is tested using TCSA numerical data in subsection 5.1.1.

However, we already know that even (3.16) is inconsistent with the proper finite size description, which gives (3.11,3.12) to leading order in λ . The underlying reason is that *the density of two-particle states is not a product of the densities of one-particle states*: the presence of the background phase shift modifies it by terms of order L^{-1} already at order λ^0 . As previously, we continue to neglect residual finite size corrections (i.e. those that decrease exponentially with the volume), but all power-like corrections must be taken into account (at least to the necessary order in λ) in order to maintain consistency.

To determine the correct normalization of the states $|A_1(p_1)A_1(p_2)\rangle$ let us introduce the total momentum $P = p_1 + p_2$ and the relative momentum $p = (p_1 - p_2)/2$. The Jacobian of this change of variables is 1 and so (in infinite volume)

$$\langle A_1(p'_1)A_1(p'_2) | A_1(p_1)A_1(p_2) \rangle = (2\pi)^2 \delta(P - P') \delta(p - p') \sqrt{p_1^2 + m_1^2} \sqrt{p_2^2 + m_1^2}$$

In finite volume, the density of states in the relative momentum variable can be obtained from the quantization condition (written here for the case of zero momentum ie. $p_1 =$

$-p_2 = p)$

$$\begin{aligned} pL + \delta(E(p)) &= 2n\pi \\ E(p) &= 2\sqrt{p^2 + m_1^2} \end{aligned} \quad (3.17)$$

The density of states in the total momentum variable is unaffected, since the phase shift drops from the quantization of the total momentum, so it is only the density in the relative momentum of the two particles which must be modified. Let us examine the equation

$$pL + \delta(E(p)) = 2n\pi$$

Taking the derivative of this equation with respect to p , first at fixed L and then at fixed n :

$$\begin{aligned} L + \frac{d\delta(E(p))}{dp} &= 2\pi \left. \frac{\partial n}{\partial p} \right|_L \\ L + \frac{d\delta(E(p))}{dp} &= -p \left. \frac{\partial L}{\partial p} \right|_n \end{aligned}$$

We obtain that the density of states at can be expressed as

$$\frac{dn}{dp} = -\frac{1}{2\pi} p \frac{dL(p)}{dp}$$

where the derivative

$$\frac{dL(p)}{dp} = \left. \frac{\partial L}{\partial p} \right|_n$$

is exactly the inverse of

$$\frac{dp(L)}{dL}$$

that was encountered in (3.10,3.11).

Therefore the appropriate normalization of the zero-momentum two-particle state finite volume two-particle state is

$$|A_1(p)A_1(-p)\rangle_L = \frac{2}{E\sqrt{L}} \left(-\frac{1}{p} \frac{dp(L)}{dL} \right)^{1/2} |A_1(p)A_1(-p)\rangle$$

which gives

$$\begin{aligned} A(L_0) &= \frac{f_{cc}}{m_c} \\ B(L_0) &= \sqrt{\left(-\frac{1}{p} \frac{dp(L)}{dL} \right) \Big|_{L=L_0}} \frac{2f_{c11}}{m_c^{3/2}} \\ C(L_0) &= \left(-\frac{1}{p} \frac{dp(L)}{dL} \right) \Big|_{L=L_0} \left(\frac{4f_{1111}}{m_c^2} + L_0 \frac{4f_{11}}{m_c} \right) \end{aligned} \quad (3.18)$$

with $p(L)$ given by (3.17). This is now consistent with (3.11) and the result of the Breit-Wigner analysis (3.12). The numerical TCSA results of section 5 do indeed confirm the inclusion of the “improvement” factors related to the density of states in finite volume. Finally, we wish to mention that similar “improvement” factors have already been proposed by Lellouch and Lüscher for the measurement of weak decay matrix element of hadrons in [34].

4 Numerical methods

4.1 Truncated conformal space approach

In the framework of perturbed conformal field theory on a cylinder with spatial circumference L , the action (2.1) leads to the Hamiltonian

$$H = H_* + \mu \int_0^L dx \Phi(t, x) + \lambda \int_0^L dx \Psi(t, x)$$

where H_* is the conformal Hamiltonian on the cylinder. Using Euclidean time $\tau = -it$ and mapping the cylinder to the plane with

$$z = \exp\left(\frac{2\pi(\tau - ix)}{L}\right) \quad , \quad \bar{z} = \exp\left(\frac{2\pi(\tau + ix)}{L}\right)$$

we obtain

$$H = \frac{2\pi}{L} \left\{ \left(L_0 + \bar{L}_0 - \frac{c}{12}\right) + \mu \left(\frac{L}{2\pi}\right)^{1-2\Delta_\Phi} \int_0^L dx \Phi(z, \bar{z}) + \lambda \left(\frac{L}{2\pi}\right)^{1-2\Delta_\Psi} \int_0^L dx \Psi(z, \bar{z}) \right\} \quad (4.1)$$

Due to translational invariance, the conformal Hilbert space \mathcal{H} can be split into sectors characterized by the eigenvalues of the total spatial momentum

$$P = \frac{2\pi}{L} (L_0 - \bar{L}_0)$$

Truncating these spaces by imposing a cut in the conformal energy, the truncated conformal space corresponding to a given truncation reads

$$\mathcal{H}_{\text{TCS}}(n, e_{\text{cut}}) = \left\{ |\psi\rangle \in \mathcal{H} \mid (L_0 - \bar{L}_0) |\psi\rangle = n |\psi\rangle, \left(L_0 + \bar{L}_0 - \frac{c}{12}\right) |\psi\rangle = e |\psi\rangle : e \leq e_{\text{cut}} \right\}$$

The essence of the truncated conformal space approach as introduced by Yurov and Zamolodchikov [4] consists in realizing that on the space $\mathcal{H}_{\text{TCS}}(n, e_{\text{cut}})$ the Hamiltonian (4.1) becomes a finite matrix, which can be diagonalized numerically to get the finite volume spectrum of the model.

In the case of the Ising model (2.6), the Hilbert space can be written as

$$\mathcal{H} = \bigoplus_{h=0, \frac{1}{16}, \frac{1}{2}} \mathcal{V}_h \otimes \bar{\mathcal{V}}_h$$

where \mathcal{V}_h is the irreducible Virasoro representation of highest weight h made from the Verma module

$$V_h = \{L_{-n_1} \dots L_{-n_k} |h\rangle : L_0 |h\rangle = h|h\rangle\} \quad (4.2)$$

by factoring out the singular vectors. Using conformal Ward identities³, the following matrices can be computed

$$\begin{aligned} (H_0)_{ij} &= \left(\Delta_i + \bar{\Delta}_i - \frac{c}{12} \right) \delta_{ij} \\ G_{ij} &= \langle i|j\rangle \\ (B_\sigma)_{ij} &= \langle i|\sigma(1,1)|j\rangle \\ (B_\epsilon)_{ij} &= \langle i|\epsilon(1,1)|j\rangle \end{aligned}$$

where $|i\rangle$ denotes a basis of $\mathcal{H}_{\text{TCS}}(n, e_{\text{cut}})$. It is very convenient to use a basis which is directly related to the Verma module basis (4.2) which is, however, not orthonormal. Instead of performing a Gram-Schmidt orthogonalization procedure this problem can be remedied by considering the Hamiltonian

$$(H_{\text{TCSA}})_{ij} = \frac{2\pi}{L} \left\{ (H_0)_{ij} + h \frac{L^{15/8}}{(2\pi)^{7/8}} (G^{-1} B_\sigma)_{ij} + \tau L (G^{-1} B_\epsilon)_{ij} \right\}$$

which is isospectral to (4.1). We can introduce a dimensionless Hamiltonian measuring energy and length in units given by the lowest particle mass m_1 at the integrable point $\tau = 0$

$$\begin{aligned} h_{\text{TCSA}} &= \frac{2\pi}{l} \left\{ H_0 + \kappa_h \frac{l^{15/8}}{(2\pi)^{7/8}} G^{-1} B_\sigma + t \kappa_h^{8/15} l G^{-1} B_\epsilon \right\} \\ l &= m_1 L \end{aligned}$$

where we use the parameters and notations introduced in section 2.2.

The application of TCSA to perturbations of $c = 1$ free boson CFT was developed originally in [7], and its use in double sine-Gordon theory is described in detail in [23, 27], therefore we give only a brief sketch to fix our conventions. For the case of the double sine-Gordon model (2.10), the relevant Hilbert space⁴ is

$$\mathcal{H} = \bigoplus_{n \in \mathbb{Z}} \mathcal{F}_n \quad (4.3)$$

³The algorithm we used here was developed originally for the numerical work in [6], but an explicit description of (the supersymmetric extension of) the matrix element determination can be found in [35]. The only published full TCSA algorithm [5] is not suitable for the present computation because it can only be applied for low truncation levels, and is not automated enough to be scalable.

⁴We consider only states with zero topological number, since the breather states we are interested in can be found in this sector.

where

$$\mathcal{F}_n = \left\{ a_{-k_1} \dots a_{-k_n} \bar{a}_{-l_1} \dots \bar{a}_{-l_m} |n\rangle : |n\rangle = \exp\left(n\frac{\beta}{2}\varphi(0,0)\right)|0\rangle \right\}$$

where the modes of the field are defined by the expansion

$$\varphi(z, \bar{z}) = \varphi_0 - \frac{i}{\sqrt{4\pi}} \Pi \log z \bar{z} + \frac{i}{\sqrt{4\pi}} \sum_{n \neq 0} \frac{1}{n} (a_n z^{-n} + \bar{a}_n \bar{z}^{-n})$$

The matrices

$$\begin{aligned} (H_0)_{ij} &= \left(\Delta_i + \bar{\Delta}_i - \frac{c}{12} \right) \delta_{ij} \\ (V_n)_{ij} &= \frac{\langle i | \exp\left(n\frac{\beta}{2}\varphi(1,1)\right) | j \rangle}{\sqrt{\langle i | i \rangle \langle j | j \rangle}} \end{aligned}$$

can be calculated explicitly in a closed form using the algebra of the free field modes. The dimensionless Hamiltonian then reads

$$h_{TCSA} = \frac{2\pi}{l} \left\{ H_0 + \kappa_{\text{sG}}(\xi) \frac{l^{\frac{2}{1+\xi}}}{(2\pi)^{\frac{1-\xi}{1+\xi}}} \frac{1}{2} (V_2 + V_{-2}) + t \frac{l^{\frac{4+3\xi}{2+2\xi}}}{(2\pi)^{\frac{2+\xi}{2+2\xi}}} \frac{1}{2} (e^{i\delta} V_1 + e^{-i\delta} V_{-1}) \right\}$$

$l = ML$

where M is the soliton mass at the integrable point $\lambda = 0$.

In both models we only consider the sector with zero total momentum $n = 0$ which is enough to obtain the necessary numerical data. The truncation levels in both cases were such that the Hilbert space dimension ranged from a few hundred up to 3-4000 states. This limitation was put mainly by machine time used for the numerical diagonalization, but in both cases the programs are fully scalable to any truncation levels, given enough computing resources (in terms of memory and execution time). For the Ising models we used $e_{\text{cut}} = 19, \dots, 27$, while in the double sine-Gordon model the typical range was $e_{\text{cut}} = 9, \dots, 15$ for lower values of ξ and $e_{\text{cut}} = 11, \dots, 17$ for higher values (in one case we used $e_{\text{cut}} = 18$). In the case of double sine-Gordon theory, due to the choice $\delta = -\pi/2$ it is possible to project the space of states onto even and odd sectors under the \mathbb{Z}_2 symmetry of the action (2.10) given by

$$\varphi \rightarrow \frac{2\pi}{\beta} - \varphi$$

as described in [27]. This reduces the dimension of the Hilbert space with a factor of approximately 2 which makes it possible to use higher values for the truncation level. We used data from the even sector to extract the results as the choice of sector does not make much difference [27].

4.2 Testing the numerics and the validity of form factor perturbation theory

We tested the numerics by making several comparisons. First we took the integrable point, where we checked whether we get suitable agreement with the exact predictions of factorized scattering theory (masses, vacuum energy density and two-particle phase shifts).

Next, in the case of the Ising model we checked the form factor perturbation theory predictions for the mass shifts (2.3) and the S matrix correction (2.4) using the form factors calculated by Delfino et al. in [2] (available at [32]) and formulae (2.3,2.4). This allowed us to determine the range of the coupling t in which perturbation theory holds with sufficient accuracy so that we can expect reasonable agreement for the perturbatively determined decay widths (2.9) as well. The S -matrix comparison must be done carefully since formula (2.4) is valid at a constant center of mass energy. Therefore every formula must be converted from rapidity variables into the energy variable as follows. The phase shift can be extracted using

$$\delta_{\text{measured}}(E) = -L \sqrt{\left(\frac{E}{2}\right)^2 - m_1(\lambda)^2 + 2n\pi}$$

where $m_1(\lambda)$ is the mass of A_1 including the correction to first order in λ . This must be compared to

$$\delta_{\text{theoretical}}(E) = \delta_0(E) + \delta_1(E) \tag{4.4}$$

where the unperturbed phase-shift is

$$\delta_0(E) = -i \log S_{11} \left(\vartheta = 2 \operatorname{acosh} \frac{E}{2m_1} \right)$$

with m_1 denoting the mass at $\lambda = 0$ since this gives the energy dependence of the unperturbed phase-shift, and to use (2.4) it is the energy that must be kept constant. The correction term can be written

$$\delta_1(E) = -i \frac{\delta S_{ab}^{cd}(\vartheta, \lambda)}{S_{11}(\vartheta)}$$

where we can use again simply

$$\vartheta = 2 \operatorname{acosh} \frac{E}{2m_1}$$

to first order in λ .

The agreement between the mass corrections and FFPT predictions for particles A_1 and A_2 is illustrated in figure 4.1, while the S -matrix test is shown in figure 4.2. Both these tests indicated that $|t| \leq 0.005$ is a suitable choice for the range of the coupling.

For the double sine-Gordon model at $\delta = -\pi/2$ it is not possible to perform a similar test, because the mass and S matrix corrections vanish at first order in t and FFPT is not formulated to second order yet. However, the program was already thoroughly tested in previous numerical studies [23, 27]. We simply chose a range of the coupling in which the measured quantities were sufficiently close to linear dependence on t .

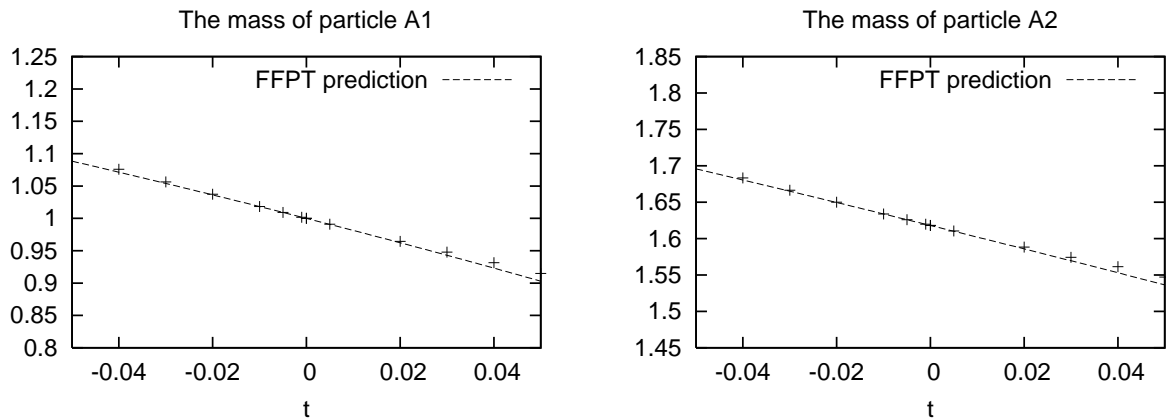


Figure 4.1: Corrections to the masses of A_1 and A_2 . TCSA data are indicated with crosses (the numerical uncertainties are too small to be displayed), while the lines give the FFPT predictions.

4.3 Numerical methods for evaluation of the decay width

We used three methods to extract the decay widths:

1. The Breit-Wigner analysis (see section 3.1.2) gives the decay rate as

$$\min \delta_1(E) - \max \delta_2(E) = 4\sqrt{-\beta\Gamma}$$

where δ_1 and δ_2 are the phase shifts extracted from the two levels using (3.5) in the vicinity of the crossing. Because we aim to extract $\sqrt{\Gamma}$ to first order in the nonintegrable coupling t , m_a and m_b in (3.5) must be substituted with the particle mass m_1 to first order in t to keep consistency to this order. Furthermore

$$\beta = \left. \frac{d\delta_0}{dE} \right|_{E=E_0} < 0$$

can be calculated using the $t = 0$ exact S -matrix for the background phase shift and $E_0 = m_c$ the $t = 0$ particle mass since any $t \neq 0$ corrections can be consistently neglected when comparing to the lowest order prediction (2.5) for the decay width Γ , from which we can extract the form factor value f_{c11} .

2. The “mini-Hamiltonian” method (section 3.1.1) when the matrix element B is extracted from the minimum energy split (3.4) between the two levels

$$\delta E(L_{\min}) = 2|B\lambda|$$

In a “naive” application of this method, we can then use the naive “mini-Hamiltonian” relations (3.16) (or, equally well, the DGM relations (3.13)) to link this directly to

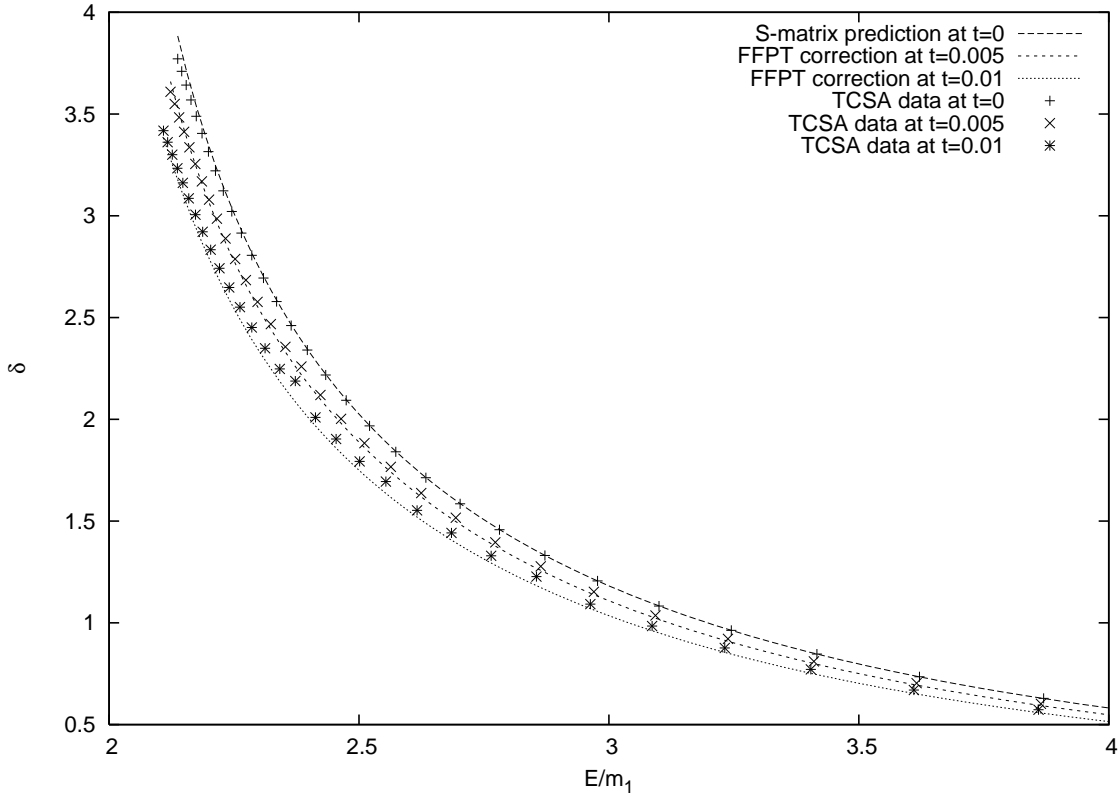


Figure 4.2: The A_1A_1 phase shift measured at $t = 0, 0.005, 0.01$ and compared to the prediction (4.4) as a function of the center of mass energy E (measured in units of the unperturbed particle mass m_1). The effect of the resonance appears on the plot as a deviation from the first order FFPT prediction (2.4) in the range around $E_c \sim m_c \approx 2.405m_1$, where a “shoulder” appears which can be observed quite clearly in the $t = 0.01$ data. It is a fine resolution scan of this “shoulder” which is used to extract the decay width when applying the Breit-Wigner method.

the three-particle form factor:

$$B_{\text{DGM}}(L_{\min}) = \frac{2f_{c11}}{\sqrt{m_c^3 L_{\min}}}$$

3. The improved “mini-Hamiltonian” method using the relations (3.18) derived in section 3.2

$$B(L_0) = \sqrt{-\frac{1}{p} \frac{dp(L)}{dL} \Big|_{L=L_{\min}}} \frac{2f_{c11}}{m_c^{3/2}}$$

Here we replaced L_0 by L_{\min} which is valid to leading order in t . In addition, the state density correction factor can be computed from

$$pL + \delta_{t=0}(E(p)) = 2n\pi$$

where $\delta_{t=0}$ is the phase shift at the integrable point $t = 0$, again to leading order in t .

In each of these approaches, the numerical setting is very convenient since the task is to find extrema of definitely convex or concave functions (the level splitting as a function of the volume or the phase shift as a function of energy). Therefore it is not even necessary to find the level crossing volume L_0 very precisely: any simple algorithm converges very fast even if the initial range given to start the search for extremum is quite wide. The background phase shift is given by (2.8) for the Ising and by (A.5) for the double sine-Gordon model. Both give phase shifts monotonically decreasing with energy (in fact any two-particle scattering phases built as products of blocks $\{x\}$ with $0 \leq x \leq 1$ automatically possess this property).

It is expected that the Breit-Wigner method should match the improved mini-Hamiltonian method as long as the resonance is narrow enough for the arguments of section 3.1.3 to apply.

4.4 Systematic errors

Contrary to the situation e.g. in lattice field theory, there are no significant sources of statistical errors. The TCSA Hamiltonian matrices are diagonalized numerically with double (16 digits) precision, and any error in calculating their spectra can be considered minuscule. There are, however, systematic errors in the extracted decay widths because (1) the TCSA Hamiltonian is not the exact one of the finite size system and (2) the analysis in Section 3 neglected residual finite size corrections (i.e. those that decay exponentially with the volume).

The first source goes by the name “truncation errors”, which originate from the fact that TCSA neglects an infinite tower of states lying above the truncation level, and grow with the volume. In the region close to a line crossing they manifest themselves most prominently in the fact that even for $t = 0$ the degeneracy is generally not exact. This can

be modeled in the “mini-Hamiltonian” picture by adding a correction matrix representing the truncation errors to (3.43.2)

$$H = E_0 + (L - L_0) \begin{pmatrix} \alpha_1 & \\ & \alpha_2 \end{pmatrix} + \lambda \begin{pmatrix} A(L) & B(L) \\ B(L) & C(L) \end{pmatrix} + \begin{pmatrix} \delta E_0 + a & b \\ b & \delta E_0 - a \end{pmatrix} \quad (4.5)$$

As a result, the minimal splitting changes to

$$\delta E(L_{\min}) = 2|b + B\lambda| = 2|B(\lambda - \lambda_0)| \quad (4.6)$$

but B can still be read out from the slope of the dependence of $\delta E(L_{\min})$ on λ and the form factor amplitude f_{c11} can then be determined from

$$B = \frac{2f_{c11}}{\sqrt{m_c^3 L_0}}$$

or

$$B = \sqrt{-\frac{1}{p} \frac{dp(L)}{dL} \Big|_{L=L_0}} \frac{2f_{c11}}{m_c^{3/2}}$$

depending on whether we use the naive or improved “mini-Hamiltonian” method, respectively.

This effect is demonstrated in figure 4.3, where it is obvious that the residual splitting decreases with increasing truncation level and gives an idea of how precise the effective description (4.5) really is. The effect of the other parameter a is to shift the value of L_{\min} while δE_0 is the truncation error in determining the resonant energy E_0 .

It is easy to see that the same modification must be performed when applying the Breit-Wigner method, and relation (3.6) must be altered as

$$\min \delta_1(E) - \max \delta_2(E) = 4|B'(\lambda - \lambda_0)|$$

from which the form factor amplitude f_{c11} for the process $A_c \rightarrow A_a + A_a$ can be read off using

$$B' = \sqrt{-\frac{d\delta_0}{dE} \Big|_{E=E_0}} \frac{f_{c11}}{m_c m_1^{1/2} \left(\left(\frac{m_3}{2m_1} \right)^2 - 1 \right)^{1/4}}$$

In the sine-Gordon case, numerics always yields $\lambda_0 = 0$ i.e. there is no residual splitting between the numerically determined levels at the integrable point. The reason is that the sine-Gordon spectrum is unaffected by $\lambda \rightarrow -\lambda$ since this can be implemented by shifting $\varphi \rightarrow \varphi + 2\pi/\beta$ in the action (2.10) and this symmetry is respected by the truncation procedure, so the numerical spectrum is even in λ (up to very small errors in numerical matrix diagonalization).

For a fixed value of e_{cut} and a choice of level crossing, we can then determine a value for f_{c11} . Then the next task is to extrapolate the results to infinite truncation level and then eliminate finite size effects (extrapolate to infinite volume).

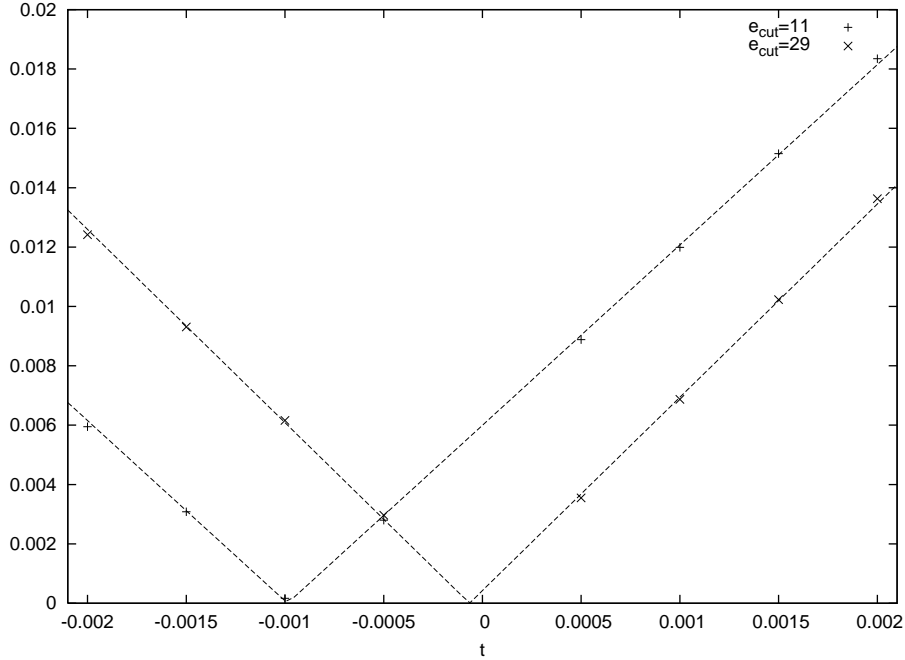


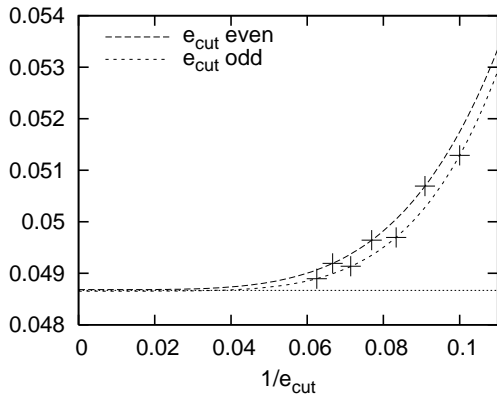
Figure 4.3: The Breit-Wigner phase shift splitting $\min \delta_1(E) - \max \delta_2(E)$ as a function of the dimensionless coupling t in the Ising case for e_{cut} values of 11 and 29.

Since truncation errors grow with increasing volume while finite size errors become larger with decreasing volume, some compromise must be struck in between. Masses are normally measured by finding the region where the measured gap is closest to being constant (has a minimum slope) and taking the value of the gap there. Two-particle phase shifts are measured over an extended volume range, and so they are affected by truncation errors at small, and by finite size errors at large values of the center of mass energy, and therefore it is very hard to perform any sort of optimization (except for a choice of the two-particle level used to extract the phase shift). Decay widths are measured in small regions around level crossings, and we perform the measurement on the first few of them, for several different values of e_{cut} .

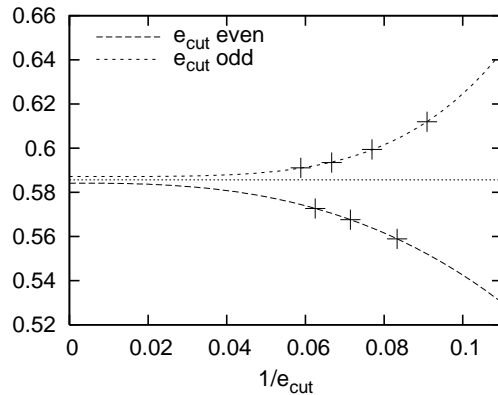
Truncation errors can be improved by fitting the truncation level dependence by some function for extrapolation to $e_{\text{cut}} = \infty$. Detailed examination of numerical data shows that they can be fit in most cases by a function of the sort

$$f(e_{\text{cut}}, L) = f(L) + a(L)e_{\text{cut}}^{-x} \quad (4.7)$$

where $f(L)$ is the extrapolated value of the measured physical quantity f at volume L , and the second terms describes the truncation effects with a and the exponent $x > 0$ to be determined from the fit. Such an extrapolation was used in [36] where it proved very useful in the determination of vacuum expectation values. Experimenting with this technique in cases where a theoretical prediction for the measured quantity is available



(a) improved "mini-Hamiltonian" method,
 $R = 2.5$



(b) Breit-Wigner method, $R = 1.7$

Figure 4.4: Truncation level extrapolation for s_{311} in the double sine-Gordon model (R is related to ξ via $2R^2 = 1 + \xi^{-1}$)

shows that this really helps, and in many cases the truncation errors are improved by an order of magnitude. Based on the numerical results the exponent x can be supposed to be independent of the coupling t and depends only very mildly on L (in the sine-Gordon case, however, a dependence on the parameter ξ must be taken into account). For an illustration see figure 4.4 which shows that separate extrapolation is necessary for odd and even values of the truncation level. The reason is that only when increasing the truncation level by a step of 2 we get new vectors in *each* (Verma or Fock) module: since the momentum is zero, we must increase the descendent quantum numbers on both left and right by 1, and thus it is only consistent to group together data pertaining to e_{cut} that differ in steps of 2. In the sine-Gordon case the situation is further complicated by the fact that the number of Fock modules \mathcal{F}_n contributing states in (4.3) also grows with the truncation level, but this effect turns out to be numerically irrelevant.

Unfortunately, there is no theoretical method providing a reliable estimate of truncation errors. However, in the case of the double sine-Gordon model the two Breit-Wigner extrapolation curves approach the average value from the two sides (as in figure 4.4 (b)) and therefore residual truncation errors can be estimated by the difference between the two extrapolated values. We adopt the same procedure for the "mini-Hamiltonian" methods as well, although in that case the situation is less clear-cut because the two sets of data approach the extrapolated limit from the same side. In the case of the Ising model, the even/odd extrapolations approach the final value from the same side for both methods, so the difference between is less reliable as an estimate for the truncation errors.

The other source of systematic errors is *residual* finite size corrections originating from vacuum polarization and the finite range of interactions. According to Lüscher's result [30, 31] these are suppressed by a factor of the form $\exp(-ML)$ where M is some characteristic

mass scale (typically the mass of the lightest particle). Such effects are e.g. the volume dependence of the particle masses and vacuum (Casimir) energy. These were neglected in all the considerations in Section 3, where the only finite size effects taken into account are the ones that decay as a power (generally L^{-2}) of the volume.

Having taken care of truncation errors, residual finite size corrections can in principle be suppressed by fitting an appropriate extrapolation function. Suppose that the decay width can be calculated from several crossings which take place in very small regions around different values of the volume L_1, \dots, L_n and that truncation errors in these determinations can be kept suitably small. Using our general understanding of finite size effects, we can think of the decay form factor f_{c11} determined at a crossing at L_i as the value of a function $f_{c11}(L)$ at $L = L_i$ with the property that

$$f_{c11}(L) = f_{c11} + O(e^{-ML})$$

where f_{c11} is the value predicted by the infinite volume quantum field theory. Unfortunately our numerical results (even after extrapolation in the truncation level) do not have sufficient precision to fit the exponential term in a reliable way. Therefore we will not perform this extrapolation in the sequel, and restrict ourselves to quoting the values of f_{c11} as measured at each level crossing separately in the Ising case; in the sine-Gordon case truncation errors allowed us to use only the first level crossing, i.e. the one that occurs at the smallest value of the volume.

5 Results

5.1 Ising model

5.1.1 Testing the mini-Hamiltonian coefficient C

It is interesting to check whether the improved “mini-Hamiltonian” description (3.18) is consistent with the numerical data. The correct formula for B can be tested by comparing the results for the decay width extracted using the Breit-Wigner method, and will be performed in subsection 5.1.2 below. Here we perform a quick test for the coefficient C . Let us take the sum of the two energy levels $E_1(L) + E_2(L)$ at the volume where the level crossing occurs at $\lambda = 0$. Then using the results of subsection (3.1.3) this must be equal to

$$E_1(L_0) + E_2(L_0) = 2m_c + \lambda(A(L_0) + C(L_0))$$

when taken at $L = L_0$ where L_0 is the volume where the levels cross. Using TCSA data with truncation level $e_{\text{cut}} = 27$, we measured this energy at five different values of the integrability breaking coupling $t = -0.003, -0.001, 0, 0.001, 0.003$, at the the first three level crossing. The results were then fitted by a linear function, parameterized as

$$\frac{E_{11}(L_0) + E_c(L_0)}{m_1} = a + bt$$

L_0	Numerics (TCSA)		“mini-Hamiltonian” prediction		
	a	b	b (DGM)	b (naive)	b (improved)
18.152	4.52877	-3.598	-0.509	-3.580	-3.974
24.900	4.80039	-4.348	-0.947	-4.016	-4.364
34.184	4.81197	-4.586	-1.263	-4.334	-4.616

Table 5.1: Testing the effect of the disconnected term and the finite volume state density factor on the “mini-Hamiltonian” description. We compare the TCSA data to three alternatives: the DGM result (3.13), the naive “mini-Hamiltonian” (3.16) and the improved version (3.18). Due to residual finite size effects, the comparison between the naive and the improved “mini-Hamiltonian” at the first level crossing cannot be taken seriously.

and are summarized in table 5.1. The theoretical value of a is

$$a = \frac{2m_4}{m_1} = 4.80973\dots$$

It is obvious that to get agreement with the TCSA results, both the disconnected term and the correct finite volume normalization of two-particle states must be taken into account. Another important point is that residual finite size effects are largest at the first level crossing, where $a = 4.52877$ is quite far from the theoretical value, therefore one cannot distinguish between the naive and the improved “mini-Hamiltonian” methods. On the other hand, the results at the other two level crossings show that both the disconnected terms and the improvement is needed in order to get appropriate agreement with the numerical data.

5.1.2 Decay widths

We measured decay width for the process $A_4 \rightarrow A_1 + A_1$ at three level crossings, while $A_5 \rightarrow A_1 + A_1$ was measured at one level crossing. We extracted the form factor matrix elements f_{411} and f_{511} using all the three methods (“naive” mini-Hamiltonian – equivalent with the DGM one for the case of the decay width–, improved mini-Hamiltonian and Breit-Wigner method) and the end results (after truncation level extrapolation) are presented in tables 5.2 and 5.3.

From table 5.2 we can see that indeed it is the improved “mini-Hamiltonian” method (rather than the naive one) which is consistent with the Breit-Wigner approach. It is also apparent that the extracted values do change with the volume, and that the naive “mini-Hamiltonian” method significantly overshoots the theoretical prediction, while both the improved “mini-Hamiltonian” and Breit-Wigner methods are in reasonable agreement with it (within 1% at the 3rd level crossing).

In the case of the matrix element f_{511} truncation errors are expected to be higher because the levels lie much higher in the spectrum. This observation is borne out by the data presented in table 5.3, where we gave the data at the two largest values of e_{cut} instead

n	$m_1 L_0$	naive mH (o/e)	improved mH (o/e)	Breit-Wigner (o/e)
1	18.152	37.658/37.662	33.422/33.426	33.255/33.336
2	24.900	38.871/38.939	35.736/35.799	34.574/34.887
3	34.184	39.099/*	36.829/*	36.318/*

Table 5.2: The measured values of f_{411} where n is the label of the level crossing, L_0 is the place of the level crossing for $t = 0$ and the last three columns give the result extracted using the method indicated at the top. The two numbers given are the extrapolated values in the truncation level for $e_{\text{cut}} = \text{odd/even}$ (*s indicate the cases where the data could not be reliably extrapolated). The theoretical prediction is $f_{411} = 36.730$.

n	$m_1 L_0$	naive mH (27/28)	improved mH (27/28)	Breit-Wigner (27/28)
1	23.206	21.011/21.120	20.244/20.349	18.551/18.612

Table 5.3: The measured values of f_{511} at the first level crossing. L_0 is the place of the level crossing for $t = 0$ and the last three columns give the result extracted using the method indicated at the top. The theoretical prediction is $f_{511} = 19.163$. Data at the second and higher crossings already have too large truncation errors. Some of the data could not be extrapolated in the truncation level; therefore we only quote the values measured at $e_{\text{cut}} = 27$ and 28.

of extrapolating them in the truncation level, because in most cases the extrapolation function (4.7) could not be fitted in a reliable way. The variation of the primary quantities $\Delta\delta$ used in the Breit-Wigner method and the minimum energy split used in both mini-Hamiltonian methods as a function of t also shows much larger t^2 effects (but decreasing t is not possible beyond a certain limit because of the presence of the residual line splitting 4.6). Therefore the matching between the Breit-Wigner and the improved “mini-Hamilton” methods is less precise, but the latter is still somewhat closer to the Breit-Wigner result than the naive version. Despite the much higher errors the two best estimates 20.349 (from the improved “mini-Hamiltonian” method) and 18.612 (from the Breit-Wigner method) are still within a few percent of the theoretical value 19.163.

5.2 Double sine-Gordon model

For convenience, we parameterize the sine-Gordon coupling as follows

$$\beta = \frac{\sqrt{4\pi}}{R} \quad , \quad \xi = \frac{1}{2R^2 - 1}$$

In table 5.4 we compare the measured values of s_{311} (see eq. (2.13)) for the three methods with the predictions, using the first level crossing (for a plot, see figure 5.1). For the “mini-Hamiltonian” methods, the values in the table are the averages of the two separate extrapolations for $e_{\text{cut}} = \text{even/odd}$, while the errors shown are the estimated residual

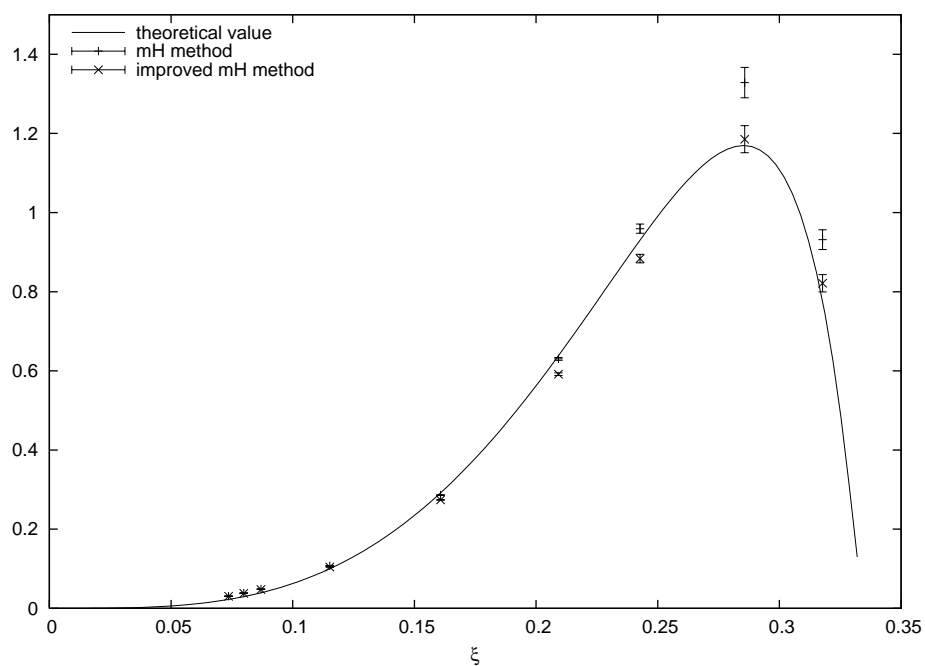


Figure 5.1: The theoretical value of s_{311} plotted against ξ , together with the numerical results obtained with the naive and the improved “mini-Hamiltonian” methods (Breit-Wigner data are omitted, since they are not significantly different from the latter). The error bars include only the residual truncation errors (the residual finite size errors are not estimated).

R	nmH	imH	BW (e/o)	FFPT	ML_0	$e^{-m_1 L_0}$
1.44	0.931 ± 0.025	0.821 ± 0.021	*/*	0.7759	16.469	10^{-7}
1.5	1.328 ± 0.038	1.185 ± 0.034	*/*	1.1694	12.398	$2 \cdot 10^{-6}$
1.6	0.959 ± 0.012	0.883 ± 0.011	0.904/0.893	0.9303	11.588	0.0002
1.7	0.630 ± 0.004	0.592 ± 0.003	0.584/0.587	0.6383	11.927	0.0005
1.9	0.286 ± 0.001	0.274 ± 0.001	*/0.269	0.2917	13.615	0.0011
2.2	0.1076 ± 0.0002	0.1046 ± 0.0002	0.110031/0.110031	0.0999	17.475	0.0018
2.5	$0.04867 \pm 2 \cdot 10^{-5}$	$0.04767 \pm 2 \cdot 10^{-5}$	*/0.049951	0.0392	22.309	0.0023
2.6	$0.03845 \pm 6 \cdot 10^{-5}$	$0.03773 \pm 6 \cdot 10^{-5}$	0.041271/0.041283	0.0295	24.089	0.0024
2.7	$0.03075 \pm 5 \cdot 10^{-5}$	$0.03022 \pm 5 \cdot 10^{-5}$	0.033467/0.033403	0.0224	25.946	0.0025

Table 5.4: Measured values of s_{311} using the “mini-Hamiltonian” and Breit-Wigner methods. The column label “nmH” corresponds to the naive, while “imH” to the improved “mini-Hamiltonian” method. The next column contain the results of the Breit-Wigner method extrapolated for even/odd truncation levels, respectively, which also give a relatively good estimate of residual truncation errors. FFPT labels the theoretical prediction, and the last two columns contain the volume corresponding to the level crossing at $t = 0$ and the characteristic suppression factor of the leading finite size correction. The *’s label the cases where the Breit-Wigner data could not be extrapolated meaningfully in the truncation level.

truncation errors calculated dividing the difference of the two extrapolated values by 2. Because the truncation level extrapolation for the Breit-Wigner method is more problematic (at least for some values of R), we show the results for even/odd truncation levels separately. Truncation errors increase with decreasing R , and indeed this is most prominently shown by the relative deviation of the measured and theoretical value at $R = 1.44$ where the Breit-Wigner method is not applicable due to the fact that albeit theoretically the condition of the monotonous decrease of the background phase shift

$$\frac{d\delta_0}{dE} < 0$$

is still satisfied, the numerical data fail to have this property. In addition, the value of L_0 for $R = 1.44$ is also significantly larger than for $R = 1.5$, which increases truncation errors too. For larger R the deviation between TCSA numerics and FFPT seems to be controlled by the residual finite size effects. Higher level crossing show too large truncation effects, and are not useful for numerical analysis. Therefore there are not enough data to estimate the residual finite size effects, and to get some idea of their magnitude we quote the exponential suppression factor characterizing their decay with the volume. Note that this is not a very precise estimate since there must certainly be additional dependence on ξ and on some power of L_0 , the form of which is not known. However, it captures the tendency correctly: the residual finite size corrections increase with R , again making the measurements at higher values of R less precise.

It is also obvious that the improvement of the “mini-Hamiltonian” method is most important for smaller R and for $R = 1.5 \dots 1.9$ it is required to get appropriate agreement with the Breit-Wigner method. For larger values of R the improvement is too small to draw any useful distinction between the naive and the improved methods. At $R = 1.44$ we see that despite the problems with the Breit-Wigner method, the improved “mini-Hamiltonian” method is still applicable and is in reasonable agreement with the theoretical prediction (relative deviation 6%), while the naive (DGM) version is again off the mark with a relative deviation of 20%.

On the other hand, note that the deviations in the range $R = 1.44 \dots 2.2$ obtained at the *first* level crossing are comparable in magnitude to those obtained in the case of the Ising model for the process $A_4 \rightarrow A_1 + A_1$ at the *second* level crossing and so we consider the agreement with the theoretical predictions fully satisfactory.

6 Conclusions and outlook

In this paper we investigated the signatures of resonances in finite volume quantum field theory. The central result of the paper is the development of two methods: (a) the Breit-Wigner method utilizing the standard parameterization of the resonant contribution to the two-particle phase shift, and (b) the improved “mini-Hamiltonian” method based on the explicit Hamiltonian description of quantum field theory, to extract (partial) decay widths of particles given the finite volume spectrum.

We have shown the equivalence between these methods to first order in the resonance width (i.e. for narrow resonances). As a further result of this investigation, we now have a finite size description of the resolution of level crossings which brings Lüscher’s description of finite size effects, the Breit-Wigner parameterization of resonances, the “mini-Hamiltonian” method and form factor perturbation theory together in a consistent framework.

Both methods are extremely simple to implement numerically since all what is needed is to find a minimum/maximum of some convex/concave function (the level splitting as a function of the volume or the phase shifts extracted from the two levels as a function of energy). However, the Breit-Wigner method does not seem to be as robust numerically under extrapolation in the truncation level (i.e. the UV cut-off) as the improved “mini-Hamiltonian” method, so the latter appears to be preferable.

Using the machinery available in the realm of 1+1 dimensional quantum field theories, namely form factor perturbation theory and truncated conformal space approach we demonstrated the efficiency of these methods, by showing agreement between the numerically extracted decay matrix elements and the theoretical ones in many cases up to a precision of 1 to 7% (as shown in figure 5.1). The most important factor in achieving this level of precision this is that both methods measure directly effects proportional to $\sqrt{\Gamma}$ (where Γ is the resonance width) in contrast to other methods proposed in the literature (such as the “plateau slope” method in [8]) which attempt to detect effects of order Γ . Therefore, our methods are much more sensitive when the resonance is narrow. Another

important advantage of methods (a) and (b) is that they only need data from a small vicinity of the level crossings resolved by the finite width of the resonance, while (as discussed at the end of subsection 3.1.2) fitting a Breit-Wigner shape directly to the extracted phase shift is not as reliable because it uses data from an extended range of the volume (containing two subsequent level crossings), and the residual finite size effects introduce significant distortion in the shape of the resonance curve.

It is clear that since the necessary description of finite size effects exists in arbitrary dimensions [31, 30, 8], the development of the two methods in Section 3 can be generalized to any number of space-time dimensions in a straightforward way and the results of the present work can be extended to more interesting theories formulated e.g. on the lattice. We remark that even the form factor approach to the calculation of the decay width has its $3+1$ dimensional counterpart in the description of the weak decays of hadrons, where the appropriate form factor is the hadronic matrix element of the weak current. The crucial issue is whether the necessary precision in the measurement of finite size effects can be attained. Therefore the most important open problem is to extend these results to theories in physical $(3+1)$ space-time dimensions, and in particular to phenomenologically relevant models.

Acknowledgments

G.T. would like to thank Z. Bajnok for useful discussions and for drawing attention to paper [2]. This work was partially supported by the EC network ‘‘EUCLID’’, contract number HPRN-CT-2002-00325, and Hungarian research funds OTKA T043582, K60040 and TS044839. G.T. was also supported by a Bolyai János research scholarship.

A The 311 form factor

In this paper we only calculate the decay width for the simplest possible case $B_3 \rightarrow B_1 + B_1$. In order to accomplish this, we need the form factor of the perturbing field $\Psi = \cos\left(\frac{\beta}{2}\Phi + \delta\right)$

$$F_{311}^\Psi(\vartheta_1, \vartheta_2, \vartheta_3) = \langle 0 | \cos\left(\frac{\beta}{2}\Phi + \delta\right) | B_3(\vartheta_1) B_1(\vartheta_2) B_1(\vartheta_3) \rangle$$

In [37] Lukyanov obtained a closed expression for the form factors of exponential operators with any number of B_1 -s in the asymptotic state. It can be written as an expectation value

$$F_{1\dots 1}^a(\vartheta_n, \dots, \vartheta_1) = \langle 0 | \exp(ia\Phi) | B_1(\vartheta_n) \dots B_1(\vartheta_1) \rangle = \mathcal{G}_a \langle \Lambda(\vartheta_n) \dots \Lambda(\vartheta_1) \rangle$$

where

$$\Lambda(\vartheta) = \frac{\bar{\lambda}(\xi)}{2 \sin \pi \xi} \left(e^{-i\frac{a\pi\xi}{\beta}} e^{-i\omega(\vartheta+i\frac{\pi}{2})} - e^{i\frac{a\pi\xi}{\beta}} e^{i\omega(\vartheta-i\frac{\pi}{2})} \right)$$

$$\bar{\lambda}(\xi) = 2 \cos\left(\frac{\pi\xi}{2}\right) \sqrt{2 \sin\left(\frac{\pi\xi}{2}\right)} \exp\left(-\int_0^{\pi\xi} \frac{dt}{2\pi} \frac{t}{\sin t}\right)$$

and the expectation value can be computed using Wick's theorem for the generalized free field ω (in a multiplicative form) with

$$\begin{aligned} \langle e^{i\alpha\omega(\vartheta)} \rangle &= 1 \\ \langle \prod_{j=1}^N e^{i\alpha_j\omega(\vartheta_j)} \rangle &= \prod_{j=1}^{N-1} \prod_{k=j+1}^N R(\vartheta_k - \vartheta_j)^{\alpha_k\alpha_j} \end{aligned}$$

where

$$\begin{aligned} R(\vartheta) &= \mathcal{N} \exp \left\{ 8 \int_0^\infty \frac{dt \sinh t \sinh t\xi \sinh t(1+\xi)}{t \sinh^2 2t} \sinh^2 t \left(1 - \frac{i\vartheta}{\pi} \right) \right\} \\ \mathcal{N} &= \exp \left\{ 4 \int_0^\infty \frac{dt \sinh t \sinh t\xi \sinh t(1+\xi)}{t \sinh^2 2t} \right\} \end{aligned} \quad (\text{A.1})$$

(the integral representation is only valid in the strip $-2\pi + \pi\xi < \Im m\vartheta < -\pi\xi$) is the so-called minimal $B_1 B_1$ form factor satisfying

$$\begin{aligned} R(-\vartheta) &= S_{11}(\vartheta)R(\vartheta) \\ R(-i\pi + \vartheta) &= R(-i\pi - \vartheta) \end{aligned} \quad (\text{A.2})$$

where $S_{11}(\vartheta)$ is the $B_1 - B_1$ two-particle scattering amplitude. Furthermore

$$\begin{aligned} \mathcal{G}_a(\beta) = \langle e^{ia\Phi} \rangle &= \left[\frac{M\sqrt{\pi}\Gamma\left(\frac{4\pi}{8\pi-\beta^2}\right)}{2\Gamma\left(\frac{\beta^2/2}{8\pi-\beta^2}\right)} \right]^{\frac{a^2}{4\pi}} \\ &\times \exp \left\{ \int_0^\infty \frac{dt}{t} \left[\frac{\sinh^2\left(\frac{a\beta}{4\pi}t\right)}{2\sinh\left(\frac{\beta^2}{8\pi}t\right)\cosh\left(\left(1-\frac{\beta^2}{8\pi}\right)t\right)\sinh t} - \frac{a^2}{4\pi}e^{-2t} \right] \right\} \end{aligned} \quad (\text{A.3})$$

is the exact vacuum expectation value of the exponential field [38].

Performing the Wick contractions explicitly we obtain

$$\begin{aligned} \langle \Lambda(\vartheta_1) \dots \Lambda(\vartheta_n) \rangle &= \left(-\frac{\bar{\lambda}}{2\sin\pi\xi} \right)^n \sum_{\{\alpha_j=\pm 1\}} \left\{ \left(\prod_{j=1}^n \alpha_j e^{\alpha_j i \frac{a\pi\xi}{\beta}} \right) \times \right. \\ &\quad \left. \prod_{j=1}^{n-1} \prod_{k=j}^n R\left(\vartheta_k - \vartheta_j - (\alpha_k - \alpha_j)i\frac{\pi}{2}\right)^{\alpha_k\alpha_j} \right\} \end{aligned}$$

where the sum goes over all the 2^n possible ‘‘configurations’’ of the auxiliary variables $\alpha_j = \pm 1$. Using the identity

$$R(\vartheta)R(\vartheta \pm i\pi) = \frac{\sinh \vartheta}{\sinh \vartheta \mp i \sin \pi\xi} \quad (\text{A.4})$$

we can write

$$R\left(\vartheta_k - \vartheta_j - (\alpha_k - \alpha_j)i\frac{\pi}{2}\right)^{\alpha_k\alpha_j} = \left(1 + i\frac{\alpha_k - \alpha_j}{2}\frac{\sin\pi\xi}{\sinh\vartheta}\right) R(\vartheta_k - \vartheta_j)$$

The end result is

$$F_{1\dots 1}^a(\vartheta_1, \dots, \vartheta_n) = \mathcal{G}_a\left(-\frac{\bar{\lambda}}{2\sin\pi\xi}\right)^n P_n^a(\vartheta_n, \dots, \vartheta_1) \prod_{j=1}^{n-1} \prod_{k=j+1}^n R(\vartheta_k - \vartheta_j)$$

$$P_n^a(\vartheta_1, \dots, \vartheta_n) = \sum_{\{\alpha_j=\pm 1\}} \left\{ \left(\prod_{j=1}^n \alpha_j e^{\alpha_j i \frac{a\pi\xi}{\beta}} \right) \prod_{j=1}^{n-1} \prod_{k=j+1}^n \left(1 + i \frac{\alpha_k - \alpha_j}{2} \frac{\sin\pi\xi}{\sinh(\vartheta_k - \vartheta_j)} \right) \right\}$$

The parity properties of the form factors are determined by

$$P_n^{-a} = (-1)^n P_n^a$$

As a result we obtain

$$\langle 0 | \cos(a\Phi) | B_1(\vartheta_1) \dots B_1(\vartheta_n) \rangle = \frac{1 + (-1)^n}{2} \langle 0 | \exp(ia\Phi) | B_1(\vartheta_1) \dots B_1(\vartheta_n) \rangle$$

$$\langle 0 | \sin(a\Phi) | B_1(\vartheta_1) \dots B_1(\vartheta_n) \rangle = \frac{1 - (-1)^n}{2i} \langle 0 | \exp(ia\Phi) | B_1(\vartheta_1) \dots B_1(\vartheta_n) \rangle$$

Form factors of higher breather can be computed using the bootstrap fusion rules [9]. To obtain B_3 one can fuse 2 B_1 -s into a B_2 and then a B_1 and a B_2 into a B_3 . The fusion angles and three-particle couplings can be read off the $B_1 - B_1$ and $B_1 - B_2$ S matrices [29]

$$S_{11} = \frac{\sinh\vartheta + i\sin\pi\xi}{\sinh\vartheta - i\sin\pi\xi} \tag{A.5}$$

$$S_{12} = \frac{\sinh\vartheta + i\sin\frac{\pi}{2}\xi \sinh\vartheta + i\sin\frac{3\pi}{2}\xi}{\sinh\vartheta - i\sin\frac{\pi}{2}\xi \sinh\vartheta - i\sin\frac{3\pi}{2}\xi}$$

If the particle c occurs as a bound state of a and b then the corresponding S matrix has a pole

$$S_{ab}(\vartheta \sim iu_{ab}^c) \sim \frac{i|\gamma_{ab}^c|^2}{\vartheta - iu_{ab}^c}$$

from which we obtain (choosing the three-particle couplings real and positive)

$$u_{11}^2 = \pi\xi \quad , \quad \gamma_{11}^2 = \sqrt{2\tan\pi\xi}$$

$$u_{12}^3 = \frac{3\pi}{2}\xi \quad , \quad \gamma_{12}^3 = \sqrt{2\frac{\tan\pi\xi \tan\frac{3\pi}{2}\xi}{\tan\frac{\pi}{2\xi}}}$$

Therefore the 311 form factor can be obtained starting from a 5-particle 11111 form factor and fusing the first three B_1 particles into a B_3 . This means that the decay process

$B_3 \rightarrow B_1 + B_1$ has a non-vanishing amplitude to leading order only if $\delta \neq 0$. Indeed, for $\delta = 0$ this process (and its generalization $B_{2n+1} \rightarrow B_1 + B_1$) is entirely forbidden by the C -parity of the breathers.

Using the notation $x_j = e^{\vartheta_j}$ we get the following result for the 5-particle form factor

$$F_{11111}^a(\vartheta_1, \dots, \vartheta_5) = \mathcal{G}_a \bar{\lambda}^5 Q_{11111}^a(\vartheta_1, \dots, \vartheta_5) \prod_{j=1}^4 \prod_{k=j+1}^5 R(\vartheta_k - \vartheta_j) \quad (\text{A.6})$$

$$Q_{11111}^a(\vartheta_1, \dots, \vartheta_5) = -i[a] \left\{ [a]^4 - [a]^2 + \frac{([a]^2(\sigma_1\sigma_4 - \sigma_5) + \sigma_5)(\sigma_2\sigma_3 - 4\sigma_5 \cos^2 \pi\xi)}{\prod_{j=1}^4 \prod_{k=j+1}^5 (x_j + x_k)} \right\}$$

where the elementary symmetric polynomials σ_k are defined by the generating function

$$\prod_{j=1}^5 (x_j + x) = \sum_{k=0}^5 x^{5-k} \sigma_k$$

and

$$[a] = \frac{\sin \frac{\pi\xi a}{\beta}}{\sin \pi\xi}$$

In the following we choose $\delta = -\pi/2$ because it will be convenient later due to another Z_2 symmetry which exists at this point (and which, on the other hand, forbids every process $B_{2n} \rightarrow B_1 + B_1$ to the lowest order). Then the form factors of the perturbing field $\Psi = \sin \frac{\beta}{2} \Phi$ can be written as

$$F_{1\dots 1}^\Psi(\vartheta_1, \dots, \vartheta_n) = \langle 0 | \sin \left(\frac{\beta}{2} \Phi \right) | B_1(\vartheta_1) \dots B_1(\vartheta_n) \rangle = -i F_{1\dots 1}^{\beta/2}(\vartheta_1, \dots, \vartheta_n)$$

for n odd.

First we fuse two B_1 's to obtain the form factor F_{2111} . The relevant equation is

$$i\gamma_{11}^2 F_{2111}^\Psi(\vartheta_1, \vartheta_3, \vartheta_4, \vartheta_5) = \text{Res}_{\epsilon=0} F_{11111}^\Psi \left(\vartheta_1 + \frac{1}{2}(i\pi\xi - \epsilon), \vartheta_1 - \frac{1}{2}(i\pi\xi - \epsilon), \vartheta_3, \vartheta_4, \vartheta_5 \right)$$

The only singularity comes from the factor $R(\vartheta_2 - \vartheta_1)$ in (A.6). The residue can be calculated quite simply due to (A.2) with the result

$$\text{Res}_{\vartheta=-i\pi\xi} R(\vartheta) = \text{Res}_{\vartheta=-i\pi\xi} S_{11}(-\vartheta) R(-\vartheta) = i(\gamma_{11}^2)^2 R(i\pi\xi)$$

and we get

$$F_{2111}^\Psi(\vartheta_1, \vartheta_3, \vartheta_4, \vartheta_5) = \mathcal{G}_{\beta/2} \bar{\lambda}^5 \gamma_{11}^2 R(i\pi\xi) Q_{11111}^\Psi \left(\vartheta_1 + \frac{i\pi\xi}{2}, \vartheta_1 - \frac{i\pi\xi}{2}, \vartheta_3, \vartheta_4, \vartheta_5 \right) \times$$

$$\prod_{j=3}^4 \prod_{k=j+1}^5 R(\vartheta_k - \vartheta_j) \prod_{l=3}^5 R\left(\vartheta_l - \vartheta_1 - \frac{i\pi\xi}{2}\right) R\left(\vartheta_l - \vartheta_1 + \frac{i\pi\xi}{2}\right)$$

where $Q_{11111}^\Psi = -iQ_{11111}^{\beta/2}$

Now we fuse B_1 and B_2 into B_3

$$i\gamma_{12}^3 F_{311}^\Psi(\vartheta_1, \vartheta_4, \vartheta_5) = \text{Res}_{\epsilon=0} F_{211}^\Psi\left(\vartheta_1 + \frac{1}{2}i\pi\xi - \frac{\epsilon}{2}, \vartheta_1 - i\pi\xi + \frac{\epsilon}{2}, \vartheta_4, \vartheta_5\right)$$

Using the same tricks as above plus the identity

$$S_{11}(2i\pi\xi) = \frac{\tan \frac{3\pi\xi}{2}}{\tan \frac{\pi\xi}{2}} = \left(\frac{\gamma_{12}^3}{\gamma_{11}^2}\right)^2$$

we obtain

$$\begin{aligned} F_{311}^\Psi(\vartheta_1, \vartheta_4, \vartheta_5) &= \mathcal{G}_{\beta/2} \bar{\lambda}^5 \gamma_{11}^2 \gamma_{12}^3 R(i\pi\xi)^2 R(2i\pi\xi) \times \\ &Q_{11111}^\Psi(\vartheta_1, \vartheta_4, i\pi\xi + \vartheta_5, \vartheta_5, -i\pi\xi + \vartheta_5,) \times \\ &R(\vartheta_5 - \vartheta_4) \prod_{j=4,5} [R(\vartheta_j - \vartheta_1 + i\pi\xi) R(\vartheta_j - \vartheta_1) R(\vartheta_j - \vartheta_1 - i\pi\xi)] \end{aligned}$$

To obtain the decay rate we need

$$f_{311} = |F_{311}^\Psi(i\pi, \vartheta_c, -\vartheta_c)|$$

where the rapidity ϑ_c of the outgoing B_1 particles can be computed from

$$2 \cosh(\vartheta_c) = \frac{m_3}{m_1} = \frac{\sin \frac{3\pi\xi}{2}}{\sin \frac{\pi\xi}{2}}$$

The result can be written as

$$f_{311} = \mathcal{G}_{\beta/2} \bar{\lambda}^5 \gamma_{11}^2 \gamma_{12}^3 \mathcal{Q}_{11111}(\xi) \mathcal{R}_{311}(\xi)$$

where

$$\begin{aligned} \mathcal{Q}_{11111}(\xi) &= -Q_{11111}^\Psi(\vartheta_c, -\vartheta_c, i\pi(1+\xi), i\pi, i\pi(1-\xi)) \\ &= \frac{(1+2\cos\pi\xi)(1+2\cos\pi\xi+2\cos 2\pi\xi)}{64 \cos \pi\xi \cos^5 \frac{\pi\xi}{2}} \end{aligned}$$

and

$$\begin{aligned} \mathcal{R}_{311}(\xi) &= \left| R(i\pi\xi)^2 R(2i\pi\xi) R(-2\vartheta_c) \times \right. \\ &R(\vartheta_c - i\pi(1-\xi)) R(\vartheta_c - i\pi) R(\vartheta_c - i\pi(1+\xi)) \times \\ &\left. R(-\vartheta_c - i\pi(1-\xi)) R(-\vartheta_c - i\pi) R(-\vartheta_c - i\pi(1+\xi)) \right| \end{aligned}$$

We can make use of eq. (A.4) to shift the arguments of the $R(2\vartheta_c)$, $R(i\pi\xi)$ and $R(2i\pi\xi)$ factors into the validity range of the integral representation (A.1). The result is

$$\mathcal{R}_{311}(\xi) = \frac{1}{2} \left| \frac{\sinh 2\vartheta_c}{\sinh 2\vartheta_c - i \sin \pi\xi} \frac{\cos \pi\xi}{2 \cos \pi\xi + 1} \frac{R(\vartheta_c - i\pi(1-\xi))^2 R(\vartheta_c - i\pi)^2 R(\vartheta_c - i\pi(1+\xi))^2}{R(i\pi(\xi-1))^2 R(i\pi(2\xi-1)) R(-2\vartheta_c - i\pi)} \right|$$

For the dimensionless matrix element s_{311} we obtain

$$s_{311}(\xi) = \frac{f_{311}}{M^{\frac{\xi}{2+2\xi}}} = \tilde{\mathcal{G}}(\xi) \bar{\lambda}(\xi)^5 2 \tan \pi\xi \sqrt{\frac{\tan \frac{3\pi\xi}{2}}{\tan \frac{\pi\xi}{2}}} \mathcal{Q}_{11111}(\xi) \mathcal{R}_{311}(\xi) \quad (\text{A.7})$$

where

$$\tilde{\mathcal{G}}(\xi) = \left[\frac{\sqrt{\pi} \Gamma\left(\frac{1+\xi}{2}\right)}{2\Gamma\left(\frac{\xi}{2}\right)} \right]^{\frac{\xi}{2+2\xi}} \exp \left\{ \int_0^\infty \frac{dt}{2t} \left[\frac{\sinh\left(\frac{\xi t}{1+\xi}\right)}{\cosh\left(\frac{t}{1+\xi}\right) \sinh t} - \frac{\xi}{1+\xi} e^{-2t} \right] \right\}$$

B Extracting $\Delta\delta = \min \delta_1 - \max \delta_2$ from the “mini-Hamiltonian”

We start from the expression (3.7) for the two levels

$$E_{1,2} = m_c + A\lambda - \alpha(L - L_{\min}) \pm \sqrt{\alpha^2(L - L_{\min})^2 + B^2\lambda^2}$$

From this the phase shift functions $\delta_{1,2}$ defined in (3.5) can be expressed as functions of L

$$\delta_{1,2}(L) = -L \sqrt{\left(\frac{E_{1,2}(L)}{2}\right)^2 - m_1^2}$$

We demonstrate how to find the extremal value of $\delta_1(L)$. We solve the equation

$$\frac{d\delta_1(L)}{dL} = 0$$

by substituting $L = L_{\min} + \kappa\lambda$ and expanding in λ . The lowest non-vanishing order is λ^0 and we find the following equation for κ

$$m_c^2 - 4m_1^2 - L_0 m_c \left(\alpha - \frac{\alpha^2 \kappa}{\sqrt{B^2 + \alpha^2 \kappa^2}} \right) = 0$$

Solving this equation and substituting the solution back into δ_1 , we find that to linear order in λ

$$\min \delta_1 = -L_0 \sqrt{\left(\frac{m_c}{2}\right)^2 - m_1^2} + B\lambda \frac{\sqrt{-(m_c^2 - 4m_1^2 - 2\alpha L_0 m_c)}}{2\alpha}$$

Performing a similar calculation for δ_2 we obtain

$$\max \delta_2 = -L_0 \sqrt{\left(\frac{m_c}{2}\right)^2 - m_1^2} - B\lambda \frac{\sqrt{-(m_c^2 - 4m_1^2 - 2\alpha L_0 m_c)}}{2\alpha}$$

The difference is

$$\min \delta_1 - \max \delta_2 = B\lambda \frac{\sqrt{-(m_c^2 - 4m_1^2 - 2\alpha L_0 m_c)}}{\alpha} \quad (\text{B.1})$$

We can go further by calculating the slope of the phase shift at $\lambda = 0$. The energy of the two-particle level (the one which is not independent of L) is then

$$E = m_c - 2\alpha(L - L_0) \quad (\text{B.2})$$

Using

$$\delta_{\lambda=0}(E) = -L(E) \sqrt{\left(\frac{E}{2}\right)^2 - m_1^2}$$

we get

$$\left. \frac{d\delta_{\lambda=0}}{dE} \right|_{E=m_c} = \frac{m_c^2 - 4m_1^2 - 2\alpha L_0 m_c}{4\alpha \sqrt{m_c^2 - 4m_1^2}}$$

which must be negative for the Breit-Wigner method to apply, so eq. (B.1) makes sense. To leading order in λ $\delta_{\lambda=0}$ can be substituted with the background phase shift δ_0 and m_c with the resonance position E_0 and so we obtain

$$\min \delta_1 - \max \delta_2 = 2B\lambda \sqrt{-\frac{1}{\alpha} \sqrt{m_c^2 - 4m_1^2} \left. \frac{d\delta_0}{dE} \right|_{E=E_0}}$$

C The “mini-Hamiltonian” coefficient C

C.1 Determining C from finite size corrections

Let us calculate the shift of a two-particle level to first order in λ . For zero total momentum, the relations (3.1) can be reformulated as

$$L \sqrt{\left(\frac{E(\lambda)}{2}\right)^2 - m_1(\lambda)^2} + \delta(E(\lambda), \lambda) = 2n\pi$$

To first order in λ , we get the following equation for the energy shift δE :

$$L \frac{\frac{E\delta E}{4} - m_1 \delta m_1}{\sqrt{\left(\frac{E}{2}\right)^2 - m_1^2}} + \frac{d\delta_0(E)}{dE} \delta E + \frac{\partial \delta(E, \lambda)}{\partial \lambda} \lambda = 0$$

where E is the energy, m_1 is the particle mass and $\delta_0(E)$ is the phase shift at $\lambda = 0$, which satisfy

$$L\sqrt{\left(\frac{E}{2}\right)^2 - m_1^2} + \delta_0(E) = 2n\pi \quad (\text{C.1})$$

and δm_1 is the mass shift to first order in λ . As a result

$$\delta E = \frac{Lm_1\delta m_1 - \sqrt{\left(\frac{E}{2}\right)^2 - m_1^2} \frac{\partial\delta(E, \lambda=0)}{\partial\lambda} \lambda}{\frac{LE}{4} + \sqrt{\left(\frac{E}{2}\right)^2 - m_1^2} \frac{d\delta_0(E)}{dE}}$$

Using (2.4) we can write at the level crossing $L = L_0$ (recall that $E(L_0) = m_c$)

$$\begin{aligned} -\sqrt{\left(\frac{m_c}{2}\right)^2 - m_1^2} \frac{\partial\delta(m_c, \lambda)}{\partial\lambda} \Big|_{\lambda=0} &= ie^{-i\delta_0(m_c)} \sqrt{\left(\frac{m_c}{2}\right)^2 - m_1^2} \frac{\partial S_{11}(m_c, \lambda)}{\partial\lambda} \Big|_{\lambda=0} \\ &= m_1 \sinh \vartheta_1^{(c11)} \frac{S_{11}(-2\vartheta_1^{(c11)}) F_{1111}^\Psi(i\pi, 2\vartheta_1^{(c11)} + i\pi, 0, 2\vartheta_1^{(c11)})}{m_1^2 \sinh 2\vartheta_1^{(c11)}} \\ &= \frac{F_{1111}^\Psi(\vartheta_1^{(c11)} + i\pi, -\vartheta_1^{(c11)} + i\pi, -\vartheta_1^{(c11)}, \vartheta_1^{(c11)})}{m_c} \end{aligned}$$

From (2.3)

$$m_1\delta m_1 = \lambda F_{11}^\Psi(i\pi, 0)$$

On the other hand, using $E(L) = 2\sqrt{p(L)^2 + m_1^2}$ (with the two particles having momentum $\pm p(L)$) we get from (C.1)

$$\frac{LE}{4} + \sqrt{\left(\frac{E}{2}\right)^2 - m_1^2} \frac{d\delta_0(E)}{dE} = -\frac{pE}{4} \frac{dL}{dp} \xrightarrow{L=L_0} \frac{m_c}{4 \left(-\frac{1}{p} \frac{dp(L)}{dL}\right) \Big|_{L=L_0}}$$

and so we obtain

$$C = \left(-\frac{1}{p} \frac{dp(L)}{dL}\right) \Big|_{L=L_0} \left(\frac{4F_{1111}^\Psi(\vartheta_1^{(c11)} + i\pi, -\vartheta_1^{(c11)} + i\pi, -\vartheta_1^{(c11)}, \vartheta_1^{(c11)})}{m_c^2} + L_0 \frac{4F_{11}^\Psi(i\pi, 0)}{m_c} \right)$$

C.2 Disconnected parts of the four-particle matrix element

We need to determine the matrix element $\langle A_1(p)A_1(-p)|\Psi(0)|A_1(p)A_1(-p)\rangle_{L=L_0}$. Returning to rapidity variables and using the crossing properties of form factors we can write (in infinite volume)

$$\begin{aligned} \text{in} \langle A_1(\vartheta_3)A_1(\vartheta_4)|\Psi(0)|A_1(\vartheta_1)A_1(\vartheta_2)\rangle_{\text{in}} &= F_{1111}^\Psi(\vartheta_3 + i\pi, \vartheta_4 + i\pi, \vartheta_1, \vartheta_2) + \\ &2\pi\delta(\vartheta_1 - \vartheta_3)F_{11}(\vartheta_4 + i\pi, \vartheta_2) + \\ &2\pi\delta(\vartheta_2 - \vartheta_4)F_{11}(\vartheta_3 + i\pi, \vartheta_1) + \\ &2\pi\delta(\vartheta_1 - \vartheta_3)\delta(\vartheta_2 - \vartheta_4)\langle 0|\Psi(0)|0\rangle \end{aligned}$$

The last term can be dropped because it is related to the vacuum energy shift, but we normalized the finite volume energy levels by subtracting the ground state. In [1], the other two disconnected pieces were canceled by mass shift counter terms; however, the finite volume Hamiltonian does not contain such terms. The δ functions can be written as

$$2\pi\delta(\vartheta_1 - \vartheta_2) = 2\pi\delta(p_1 - p_2)m_1 \cosh \vartheta_1$$

and in finite volume (L_0)

$$2\pi\delta(\vartheta_1 - \vartheta_2)|_{\vartheta_1=\vartheta_2} = L_0 m_1 \cosh \vartheta_1$$

We need the matrix element at the special rapidity values $\vartheta_1 = -\vartheta_2 = \vartheta_3 = -\vartheta_4 = \vartheta_1^{(c11)}$ (recall that $m_c = 2m_1 \cosh \vartheta_1^{(c11)}$) which gives

$$\begin{aligned} \langle A_1(p)A_1(-p)|\Psi(0)|A_1(p)A_1(-p)\rangle_{L=L_0} &= F_{1111}^\Psi \left(\vartheta_1^{(c11)} + i\pi, -\vartheta_1^{(c11)} + i\pi, -\vartheta_1^{(c11)}, \vartheta_1^{(c11)} \right) + \\ & m_c L_0 F_{11}^\Psi(i\pi, 0) \end{aligned}$$

References

- [1] G. Delfino, G. Mussardo and P. Simonetti, *Nucl. Phys.* **B473** (1996) 469-508, hep-th/9603011.
- [2] G. Delfino, P. Grinza and G. Mussardo, *Nucl. Phys.* **B737** (2006) 291-303, hep-th/0507133.
- [3] C.R. Fernandez-Pousa, M.V. Gallas, T.J. Hollowood and J.L. Miramontes, *Nucl. Phys.* **B484** (1997) 609-630, hep-th/9606032.
C.R. Fernandez-Pousa and J.L. Miramontes, *Phys. Lett.* **B472** (2000) 392-401, hep-th/9910218.
O.A. Castro-Alvaredo, A. Fring, C. Korff and J.L. Miramontes, *Nucl. Phys.* **B575** (2000) 535-560, hep-th/9912196.
- [4] V. P. Yurov and Al. B. Zamolodchikov, *Int. J. Mod. Phys.* **A6** (1991) 4557-4578.
- [5] M. Lassig and G. Mussardo, *Comput. Phys. Commun.* **66** (1991) 71-88.
- [6] H. Kausch, G. Takács and G. Watts, *Nucl. Phys.* **B489** (1997) 557-579, hep-th/9605104.
- [7] G. Feverati, F. Ravanini and G. Takács, *Phys. Lett.* **B430** (1998) 264-273, hep-th/9803104.
- [8] M. Lüscher, *Nucl. Phys.* **B364** (1991) 237-254.

- [9] F.A. Smirnov: Form-factors in completely integrable models of quantum field theory, *Adv. Ser. Math. Phys.* **14** (1992) 1-208.
- [10] G. Delfino and G. Mussardo, *Nucl. Phys.* **B516** (1998) 675-703, hep-th/9709028.
- [11] M. Caselle, M. Hasenbusch, A. Pelissetto and E. Vicari, *J. Phys.* **A34** (2001) 2923-2948, cond-mat/0011305.
- [12] P. Fonseca and A. Zamolodchikov: Ising field theory in a magnetic field: analytic properties of the free energy, preprint RUNHETC-2001-37, hep-th/0112167.
- [13] P. Grinza and A. Rago, *Nucl. Phys.* **B651** (2003) 387-412, hep-th/0208016.
- [14] M. Caselle, P. Grinza and A. Rago, *J. Stat. Mech.* **0410** (2004) P009, hep-lat/0408044.
- [15] B.M. McCoy and T.T. Wu, *Phys. Rev.* **D18** (1978) 1259.
- [16] S. B. Rutkevich, *Phys. Rev. Lett.* **95** (2005) 250601, hep-th/0509149.
- [17] A.B. Zamolodchikov, *Advanced Studies in Pure Mathematics* **19** (1989) 641; *Int. J. Mod. Phys.* **A3** (1988) 743.
- [18] V.A. Fateev, *Phys. Lett.* **B324** (1994) 45.
- [19] G. Delfino and P. Simonetti, *Phys. Lett.* **B383** (1996) 450-456, hep-th/9605065.
- [20] V.A. Fateev, S. Lukyanov, A.B. Zamolodchikov and Al.B. Zamolodchikov, *Nucl. Phys.* **B516** (1998) 652.
- [21] M. Fabrizio, A.O. Gogolin and A.A. Nersesyan, *Nucl. Phys.* **B580** (2000) 647-687, cond-mat/0001227.
- [22] R.K. Bullough, P.J. Caudry and H.M. Gibbs, in Solitons, Eds. R.K. Bullough and P.J. Caudry, *Topics in Current Physics* v. **17**, Springer-Verlag, 1980.
- [23] Z. Bajnok, L.Palla, G. Takács and F. Wágner, *Nucl. Phys.* **B601** (2001) 503-538, hep-th/0008066.
- [24] G. Zs. Tóth, *J. Phys.* **A37** (2004) 9631-9650, hep-th/0406139.
- [25] G. Mussardo, V. Riva and G. Sotkov, *Nucl. Phys.* **B687** (2004) 189-219, hep-th/0402179.
- [26] J. Goldstone and R. Jackiw, *Phys. Rev.* **D11** (1975), 1486-1498.
- [27] G. Takács and F. Wágner, *Nucl. Phys.* **B**, in press, hep-th/0512265.
- [28] Al. B. Zamolodchikov, *Int. J. Mod. Phys.* **A10** (1995) 1125-1150.

- [29] A.B. Zamolodchikov and Al.B. Zamolodchikov, *Annals Phys.* **120** (1979) 253-291.
- [30] M. Lüscher, *Comm. Math. Phys.* **105** (1986) 153-188.
- [31] M. Lüscher, *Comm. Math. Phys.* **104** (1986) 177.
- [32] <http://www.sissa.it/~delfino/isingff.html>
- [33] T.R. Klassen and E. Melzer, *Nucl. Phys.* **B362** (1991) 329-388.
- [34] L. Lellouch and M. Lüscher, *Commun. Math. Phys.* **219** (2001) 31-44, hep-lat/0003023.
- [35] M. Kormos: Boundary renormalization group flows of unitary superconformal minimal models, preprint ITP Budapest Report No. 625, hep-th/0512085. *Nuclear Physics B*, in press.
- [36] Z. Bajnok, L.Palla, G. Takács and F. Wágner, *Nucl. Phys.* **B587** (2000) 585-618, hep-th/0004181.
- [37] S. Lukyanov, *Mod. Phys. Lett.* **A12** (1997) 2543-2550, hep-th/9703190.
- [38] S. Lukyanov and A.B. Zamolodchikov, *Nucl. Phys.* **B493** (1997) 571-587, hep-th/9611238.